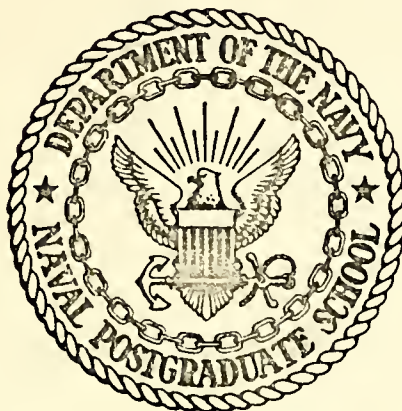


AN EXPERIMENTAL STUDY OF THE
PNEUMATIC ANGULAR RATE SENSOR

Daniel B. Mulligan

NAVAL POSTGRADUATE SCHOOL

Monterey, California



THESIS

AN EXPERIMENTAL STUDY OF THE
PNEUMATIC ANGULAR RATE SENSOR

by

Daniel B. Mulligan

Thesis Advisor:

T. Sarpkaya

June 1973

Approved for public release; distribution unlimited.

T155101

An Experimental Study of the
Pneumatic Angular Rate Sensor

by

Daniel B. Mulligan
Lieutenant, United States Navy
B.S., United States Naval Academy, 1967

Submitted in partial fulfillment of the
requirements for the degree of

MASTER OF SCIENCE IN MECHANICAL ENGINEERING

from the
NAVAL POSTGRADUATE SCHOOL
June 1973

ABSTRACT

The purpose of this investigation was to determine the response of a pneumatic angular rate sensor with two spherical pickoff elements, and to develop a suitable prototype sensor to be used in further analysis and experimentation. It was found that optimum response is obtained when the spherical elements are located within the sink tube, and that in the development of a suitable prototype, a fluid of relatively high density with low flow rates should be used to minimize system noise while retaining high system response.

TABLE OF CONTENTS

I.	INTRODUCTION -----	8
II.	DESCRIPTION OF THE APARATUS -----	11
III.	EXPERIMENTAL PROCEDURE -----	12
IV.	EXPERIMENTAL UNCERTAINTY -----	14
V.	ANALYSIS OF THE SENSOR OUTPUT -----	16
VI.	DISCUSSION OF RESULTS AND CONCLUSIONS -----	20
VII.	RECOMMENDATIONS FOR FUTURE WORK -----	23
BIBLIOGRAPHY -----		67
INITIAL DISTRIBUTION LIST -----		68
FORM DD 1473 -----		69

LIST OF FIGURES

Figure

1.	Fluid Flow in Sensor -----	24
2.	Sensor Assembly -----	25
3.	Spherical Pickoff Element Location -----	26
4.	Pickoff Elements -----	27
5.	Differential Pressure vs. Angular Velocity (summary for spherical elements) -----	28
6.	Differential Pressure vs. Angular Velocity (inserted spherical elements .87 SCFM) -----	29
7.	Differential Pressure vs. Angular Velocity (inserted spherical elements .956 SCFM) -----	30
8.	Differential Pressure vs. Angular Velocity (inserted spherical elements 1.044 SCFM) -----	31
9.	Differential Pressure vs. Angular Velocity (inserted spherical elements 1.131 SCFM) -----	32
10.	Differential Pressure vs. Angular Velocity (inserted spherical elements 1.218 SCFM) -----	33
11.	Differential Pressure vs. Angular Velocity (inserted spherical elements 1.305 SCFM) -----	34
12.	Differential Pressure vs. Angular Velocity (outside spherical elements .87 SCFM) -----	35
13.	Differential Pressure vs. Angular Velocity (outside spherical elements .956 SCFM) -----	36
14.	Differential Pressure vs. Angular Velocity (outside spherical elements 1.044 SCFM) -----	37
15.	Differential Pressure vs. Angular Velocity (outside spherical elements 1.131 SCFM) -----	38
16.	Differential Pressure vs. Angular Velocity (outside spherical elements 1.218 SCFM) -----	39
17.	Differential Pressure vs. Angular Velocity (outside spherical elements 1.305 SCFM) -----	40

18.	Differential Pressure vs. Angular Velocity (outside spherical elements 1.392 SCFM) -----	41
19.	Differential Pressure vs. Angular Velocity (cylindrical element .87 SCFM) -----	42
20.	Differential Pressure vs. Angular Velocity (cylindrical element 1.044 SCFM) -----	43
21.	Differential Pressure vs. Angular Velocity (cylindrical element 1.218 SCFM) -----	44
22.	Differential Pressure vs. Angular Velocity (cylindrical element 1.392 SCFM) -----	45
23.	Differential Pressure vs. Angular Velocity (spherical cylindrical comparison) -----	46
24.	K vs. $\omega^0 R^3/Q$ (inserted spherical elements .87 SCFM) -----	47
25.	K vs. $\omega^0 R^3/Q$ (inserted spherical elements .956 SCFM) -----	48
26.	K vs. $\omega^0 R^3/Q$ (inserted spherical elements 1.044 SCFM) -----	49
27.	K vs. $\omega^0 R^3/Q$ (inserted spherical elements 1.131 SCFM) -----	50
28.	K vs. $\omega^0 R^3/Q$ (inserted spherical elements 1.218 SCFM) -----	51
29.	K vs. $\omega^0 R^3/Q$ (inserted spherical elements 1.305 SCFM) -----	52
30.	K vs. $\omega^0 R^3/Q$ (outside spherical elements .87 SCFM) -----	53
31.	K vs. $\omega^0 R^3/Q$ (outside spherical elements .956 SCFM) -----	54
32.	K vs. $\omega^0 R^3/Q$ (outside spherical elements 1.044 SCFM) -----	55
33.	K vs. $\omega^0 R^3/Q$ (outside spherical elements 1.131 SCFM) -----	56
34.	K vs. $\omega^0 R^3/Q$ (outside spherical elements 1.218 SCFM) -----	57
35.	K vs. $\omega^0 R^3/Q$ (outside spherical elements 1.305 SCFM) -----	58
36.	K vs. $\omega^0 R^3/Q$ (outside spherical elements 1.392 SCFM) -----	59

37.	K vs. $\omega^0 R^3/Q$ (cylindrical element summary) -----	60
38.	Prototype System -----	61
39.	Prototype Pressure Sensor System -----	62
40.	Pressure Sensor Section I -----	63
41.	Pressure Sensor Section II -----	64
42.	Pressure Sensor Section III -----	65
43.	Sensor Assembly -----	66

LIST OF SYMBOLS

Q	total flow rate through the sensor, SCFS
p	pressure, lb/ft ²
U _s	average velocity in the sink tube, ft/sec
ρ	fluid density, slugs/ft ³
θ	angle from the horizontal axis of the sink tube
V _{ms}	maximum swirl velocity
ω	angular velocity, rad/sec
ω ^o	angular velocity, deg/sec
R	effective radius, ft.
r _p	radial distance to pickoff hole, ft.
r _{sph}	radius of sphere, ft.
r _c	radius of cylinder, ft.
b	disk spacing

I. INTRODUCTION

The purpose of the experimental investigation described herein is to determine the response of a pneumatic angular rate sensor with two spherical pressure-pickoff elements, and to develop a suitable prototype sensor to be used in further experimentation.

The pneumatic angular rate sensor is a device which utilizes the change in the characteristics of fluid flow, namely the swirl created by rotation, to detect the changes in motion of the system to which the sensor is rigidly attached. The detection is in the form of a pressure difference which can be translated to a rate of motion for a specified flow rate.

The sensor consists basically of two coaxial disks, spaced 1/20 to 1/50 radius apart. One disk is supported by a system of evenly spaced radial veins mounted on another coaxial disk, an outlet sink, two spherical pickoff elements, and an inlet tube located along the center axis.

The gaseous fluid flows (Fig. 1) through the inlet tube through a foam section of uniform length and porosity contained within the tube. The fluid flows uniformly and radially through the veins and around the center disk and discharges at the sink tube. The radial flow between the two coaxial disks is modified by the viscous shear and by the vortex created by the rotation of the unit about an axis

parallel to the axis of symmetry. The vortex created by the sensor rotation produces a pressure difference across the pressure sensing elements and it is this pressure difference, for a specified flow, which is directly related to the rate of rotation.

The experimental results were compared with the results of a cylindrical pickoff element, used with the same sensor, to show that the optimum system response is that of a system containing spherical elements.

Due to the increased interest in fluidic devices, a number of studies of vortex flows and vortex chambers have been performed. Sarpkaya and Kirshner [1] studied the theoretical and experimental performance characteristics of a pneumatic angular rate sensor using a cylindrical probe as a pickoff element. Later Sarpkaya [2] presented a critical discussion of the characteristics of the angular rate sensor. The fundamental problems summarized in his paper were the basis for this investigation. Richards [3] applied a numerical technique for solving the full Navier-Stokes equation to the vortex-rate sensor and found that the conditions at the sink tube affect the local flow pattern, but have little influence on the flow farther upstream. It was also shown that the velocity profiles near the sink are virtually unaffected. De Santis and Rakowsky [4] conducted an experimental investigation to determine the characteristics of flow with a weak vortex produced by the combination of radial axisymmetric sink flow and vortex flow between two

closely spaced coaxial circular plates. The experiments of Rakowsky have verified the viscous flow analysis carried out by Sarpkaya [1]. Iwadare and Hakiwara [5] made a study of the system response of the sensor used by Sarpkaya but with a variation in the type of probe tube used. Their results have shown that the noise level is relatively high and the range of response of the sensor is rather narrow.

II. DESCRIPTION OF THE APPARATUS

The system components used in the experimentation were arranged in the following manner. Air passed through a series of pipes and entered a 1.74 SFCM flow meter, where it was controlled from 0 to 100 percent of this rating, and into the inlet tube of the sensor. The sensor was mounted on a circular platform, with a horizontal axis. The circular platform was mounted on a support system which allowed the platform to be rotated. The support system was made up of three guide rollers. The platform was rotated by a drive mechanism connected to one of these guide rollers. The speed of rotation was controlled by a variable speed General Electric 1/6 horsepower motor. The rotation of the system was determined by mounting a trigger switch on the support system and locating a series of round head screws every 60 degrees on the circular platform to trigger this timing switch. The impulse from the switch was transmitted to the external time input of the Hewlett-Packard 7702 B recorder.

As air passed through the sensor and out the outlet sink, it flowed past the two spherical pressure pickoff elements. Each pickoff element was connected by a section of tubing to one side of a Sanborn 267AC pressure transducer. The transducer transferred the differential pressure of the pickoff elements to the Hewlett-Packard recorder.

Figures 2, 3, and 4 contain drawings of the sensor and the pressure pickoff elements.

III. EXPERIMENTAL PROCEDURE

The experiment was conducted in two parts: in the first part a cylindrical pressure pickoff element was used. In the second part, two spherical pressure pickoff elements were used.

The cylindrical pickoff element was positioned such that the pickoff holes were located 45 degrees both from the axis of the sink tube and from the direction of the flow in the sink tube. As discussed in the theoretical development, positioning of the holes 45 degrees from the direction of flow gives the maximum theoretical pressure difference across the pressure pickoff holes.

The cylindrical pickoff element was moved until the two pressure pickoff holes were equidistant from the center axis of the sink tube and until there was a zero pressure difference across the transducer for all the flow-rates used. The null-signal was less than 0.0014 psi for flow rates from 0.75 to 1.392 SCFM. Having established a null reference, the system was rotated at angular velocities of 0 to 55 degrees per second at various flow rates. Rotation was both clockwise and counterclockwise. The rotation produced, as would be expected, a pressure difference across the sensing element. This pressure difference was then converted by the pressure transducer to a signal which was displayed by the recorder. Knowing the calibration of the transducer,

this deflection was then used to calculate the pressure difference.

The angular velocity was determined by counting the timer signals per 360 degrees as generated by the trigger switch assembly and the recorder.

This procedure was consistant in both parts of the experiment.

The spherical pickoff elements used in the second part of the investigation were positioned such that each pickoff hole was located at a position 45 degrees from the axis of the sink tube and from the direction of flow in the sink tube. The spherical pickoff elements were moved until the exit plane of the sink tube was tangent to both spherical elements and there was a zero pressure difference across the transducer for all flow rates used.

The procedure for recording data was the same as that of the cylindrical element.

In another series of experiments the spherical elements were placed in the sink tube one diameter, (0.083 inches), from the exit plane to determine the system response at this position. The same procedure for zeroing the system and recording data was used.

IV. EXPERIMENTAL UNCERTAINTY

In the data obtained using the Hewlett-Packard recorder the differential pressure was recorded as a deflection in millimeters on the recorder chart paper. The uncertainty in this reading comes from two sources; firstly, from the inability of the observer to determine the deflection reading beyond 0.5 mm; and secondly, from the uncertainty in the calibration of the transducer.

The uncertainty occurring in the calibration of the transducer arises from the ability to read the water level and the inability to translate the deflection on the recorder of this pressure beyond 0.5 mm.

There are also two effects on the uncertainty of the angular velocity, namely, the error in the chart speed of the recorder and the inability to read the translation distance on the chart beyond 0.5 mm.

The uncertainty in reading the flow meter is the only adverse effect on the flow reading.

The three quantities determined were the pressure differential Δp expressed in psi, the sensor angular velocity ω expressed in deg/sec, and the flow rate Q expressed in SCFM.

Using the notation $\bar{\omega}_x$ as the uncertainty in x , the experimental uncertainty interval expression for p , ω , and Q are;

$$\bar{\omega}_{\Delta p} = \left[\left(\frac{\partial \Delta p}{\partial CR} \bar{\omega}_{CR} \right)^2 + \left(\frac{\partial \Delta p}{\partial T} \bar{\omega}_T \right)^2 \right]^{\frac{1}{2}}$$

and

$$\bar{\omega}_\omega = \left[\left(\frac{\partial \omega}{\partial CS} \bar{\omega}_{CS} \right)^2 + \left(\frac{\partial \omega}{\partial CR} \bar{\omega}_{CR} \right)^2 \right]^{\frac{1}{2}}$$

and

$$\bar{\omega}_Q = \left[\left(\frac{\partial Q}{\partial Q} \bar{\omega}_Q \right)^2 \right]^{\frac{1}{2}}$$

where CR = chart reading

T = transducer

CS = chart speed

Q = flow reading

After simplifying and substituting the appropriate values, the above equations yielded results which were well within the acceptable limits of experimental uncertainty. The maximum error was calculated to be 5 percent in $\Delta p/\text{deg/sec.}$

V. ANALYSIS OF THE SENSOR OUTPUT

The pressure distribution for the potential flow about a sphere is given by

$$p = \rho U_s^2 (1 - 2.25 \sin^2 \theta) / 2 \quad (1)$$

where U_s is the average velocity in the sink tube about the pickoff elements. Evidently, $dp/d\theta$ is maximum for $\theta = 45^\circ$ (for flow around a cylindrical pickoff also) and $p = 0$ for $\theta = 41.7^\circ$. It is easy to verify that the pressure varies nearly linearly from approximately $\theta = 30^\circ$ to $\theta = 60^\circ$. This is more than sufficient since the swirl angle is seldom greater than $\Delta\theta = \pm 20^\circ$ for a sensor with sufficiently low response time or high power level.

The differential pressure between the two pickoff holes is given by

$$\Delta p = \frac{9}{4} U_s^2 \rho \Delta \theta \quad (2)$$

since $\sin 2\theta = 1$ for $\theta = 45^\circ$ and 0.933 for $\theta = 41.7^\circ$. Furthermore, it is apparent that a pickoff hole placed between $\theta = 45^\circ$ and $\theta = 41.7^\circ$ on a small sphere will sample the flow over an area rather than sense it at a point. Now noting that the swirl angle, resulting from the tangential velocity of the fluid relative to the tangential velocity of the pickoff hole is given by

$$\tan \Delta\theta = \frac{V_{ms} - r_p \omega}{U_s} \quad \text{or} \quad \Delta\theta = \frac{V_{ms}}{U_s} \quad (3)$$

where V_{ms} is the maximum swirl velocity in the sink tube, and that

$$V_{ms} = \omega R^2 / r_p \quad (4)$$

where ω is the angular velocity in radians per second, R is the effective radius of the sensor, r_p the radial distance to the location of the pickoff hole which is also the radius where the tangential velocity is a maximum. Equation (2) may be reduced to

$$\Delta p = \frac{9}{4} \rho \omega R U_s \left(\frac{R}{r_p} \right) \quad (5)$$

writing $Q = U_s (\pi r_s^2 - 2\pi r_{sph}^2)$ where r_{sph} is the radius of the sphere, equation (5) reduces to

$$\Delta p = \left(\frac{9}{4\pi} \right) \left(\frac{R^2}{r_p^2} \right) \left(\frac{\rho \omega Q}{r_s^2 \left(1 - 2 \frac{r_{sph}^2}{r_s^2} \right)} \right) \quad (6)$$

for the case when the pickoff elements are placed within the sink tube. In the case where the pickoff elements are placed outside the sink tube $Q = \pi r_s^2 U_s$, i.e., very little flow blockage, one has

$$\Delta p = \frac{9}{4\pi} \frac{R^2}{r_p} \frac{\rho \omega Q}{r_s^2} \quad (7)$$

It is evident from equations (6) and (7) that the differential pressure signal increases most rapidly with decreasing sink-tube radius, secondly with increasing sensor radius, and thirdly with increasing rate of rotation, flow rate and fluid density. Obviously, there is a limit to the magnitude of each and every one of these parameters. The size of the sink-tube is limited by the size of the pickoff element which in turn is limited by the manufacturing difficulties. The flow rate is limited by the capacity of the available power source. Finally, the sensor radius is limited by the space and weight requirements and most importantly by the response-time consideration.

The response time T is proportional to bR^2/Q where b is the disk spacing. Thus to optimize the ratio of the differential pressure output to the response time, the maximum possible value of the following ratio must be sought

$$(\rho\omega Q^2)/(br_s^3) \quad (8)$$

It is apparent that the radius of the sensor does not enter into this optimization since its effect on the increase of the differential pressure is compensated by a proportional amount of increase on the response time. Thus the most optimum sensor may be obtained by decreasing the sink tube radius and the disk spacing and by increasing the flow rate for a given fluid and angular velocity. As cited earlier, all of these quantities are limited in their range by practical considerations. The dimensions of the sensor used herein were chosen with these limitations in mind.

The experimental data is compared with those predicted theoretically through the use of equations (6) and (7). These will be presented in the discussion of results. In passing, it should be noted that equation (6) may be written for convenience as follows

$$\Delta p = 0.0125 \left(\frac{R^2}{r_p} \right) \frac{\rho \omega^0 Q}{r_s^2 \left(1 - 2 \frac{r_{sph}^2}{r_s^2} \right)} \quad (9)$$

where ω^0 is now measured in degrees per second.

Finally, it should be noted that it is rather difficult to calculate flow blockage in swirling flow due to the presence of two spheres in the sink tube. For this reason, here it is assumed that the sink tube area is reduced by the projected area of the spheres in calculating the effective flow area. In fact the experiments show that this approximation is fairly correct as will be discussed later.

VI. DISCUSSION OF RESULTS AND CONCLUSIONS

The experimental results are presented in terms of the differential pressure versus the rate of rotation as shown in Figures 5 through 22. The results show that the system response is linear for each test condition. The slope of the linear response was defined as the response of the sensor and is expressed in psi/deg/sec.

The results also show that the sensor response is larger for the case where the spherical elements are located inside the sink tube. These results are consolidated in Figure 23 where each line indicates the best linear approximation to the experimental data. This figure also provides a comparison between the results of the spherical and cylindrical pickoff elements. The results were then normalized to compare them with those predicted theoretically. These normalized values, expressed in terms of K are shown in Figures 24 through 37. The parameter K is defined for the spherical elements located within the sink tube as,

$$K = \frac{\Delta p}{\left(\frac{R}{r_s}\right)^2 - \frac{\rho \omega^2 Q}{r_p \left(1 - 2 \frac{r_{sp}^2}{r_s^2}\right)}}$$

and for the spherical element located tangent to the exit plane of the sink tube as,

$$K = \frac{\Delta p}{\left(\frac{R}{r_s}\right)^2 \frac{\rho \omega^0 Q}{r_p}}$$

and for the cylindrical element as,

$$K = \frac{\Delta p}{\left(\frac{R}{r_s}\right)^2 \frac{\rho \omega^0 Q}{r_p \left(1 - \frac{4}{\pi} \frac{r_c}{r_s}\right)}}$$

K was plotted as a function of

$$\frac{\omega^0 R^3}{Q}$$

The theoretical value of K was found to be 0.0125. The experimental values obtained were in close agreement with the theoretical value and had a standard deviation of 0.0026 from the theoretical. An explanation of this deviation is that the actual area reduction must consider the effective area of a body in swirling flow, which is unknown. For this reason, an assumption that the cross-section area of the pickoff element would closely approximate the effective area reduction was made. From the results it can be seen that the theoretical prediction of the value of K is an acceptable approximation because of its close correlation with the experimental results.

It was concluded that the spherical element located within the sink tube gave the system its best response. Also the area reduction of the pickoff tube by the sensing element must be included in the theoretical development

because this area reduction has a pronounced effect on the system performance.

It was observed that the system, when exposed to the higher flow rates, displayed a significant amount of noise. It was concluded that to minimize this noise the system should be redesigned to accommodate a fluid of greater density and lower flow rates without loss of system response. Figures 38 through 43 contain this proposed design.

VI. RECOMMENDATIONS FOR FUTURE WORK

It is recommended that the proposed sensor be constructed and evaluated for the expected reduction in system noise without loss of system response. See Figures 38 through 43.

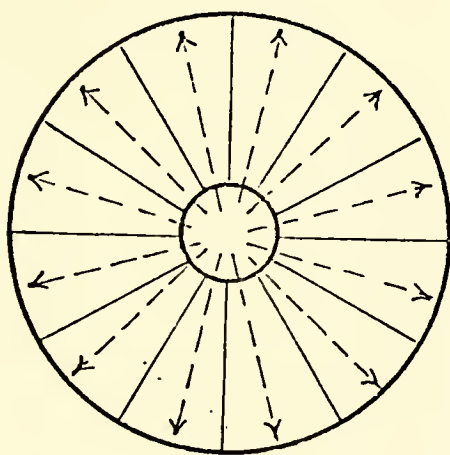
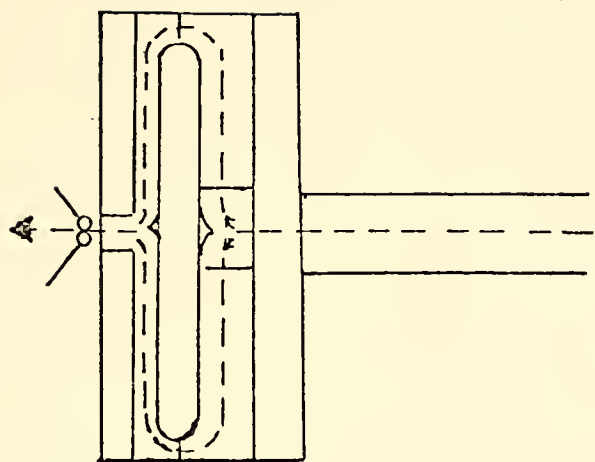


Figure 1. Fluid Flow in Sensor.

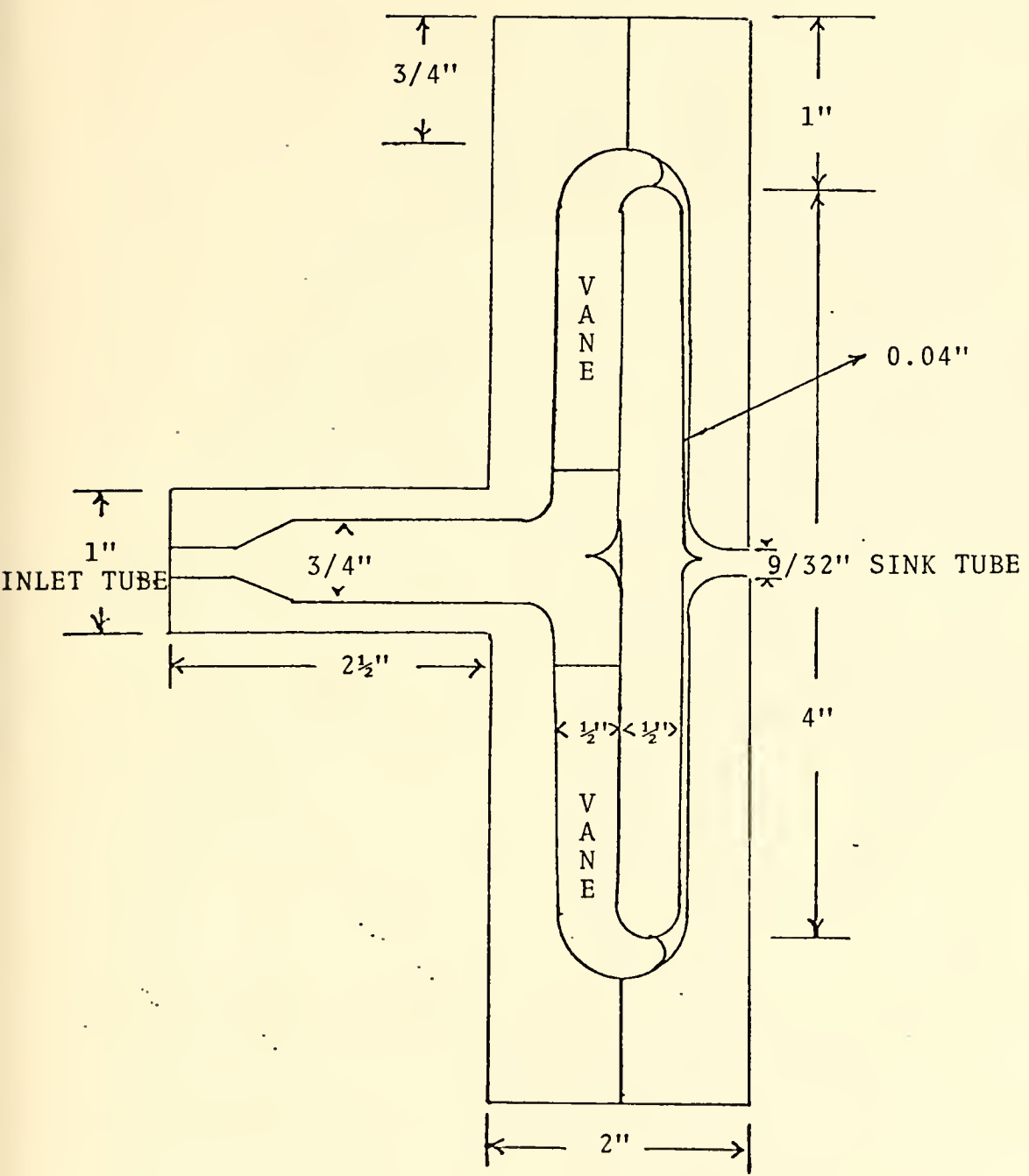


Figure 2. Sensor Assembly.

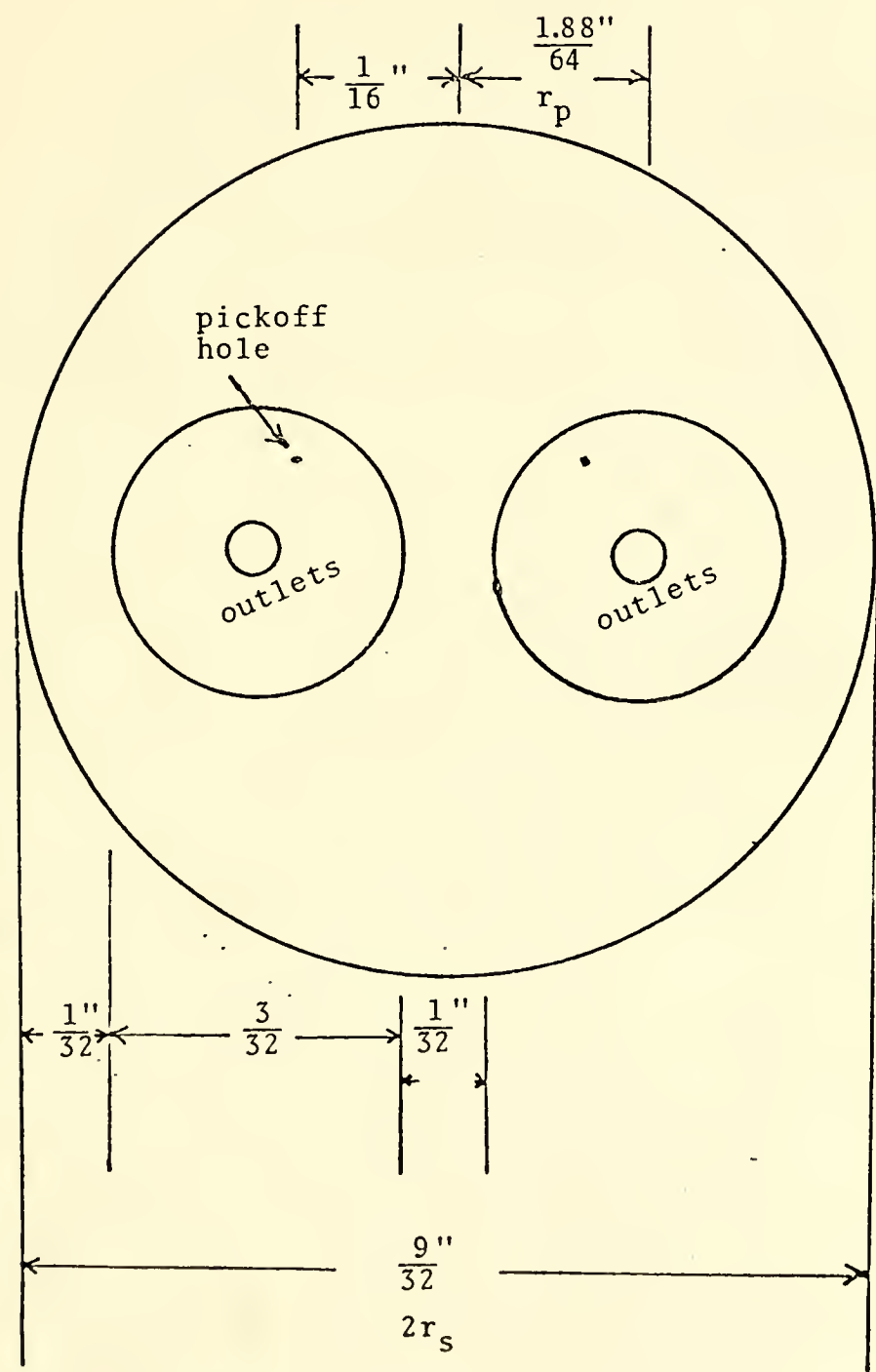


Figure 3. Spherical Pickoff Element Location.

CYLINDRICAL PRESSURE
PICKOFF ELEMENT

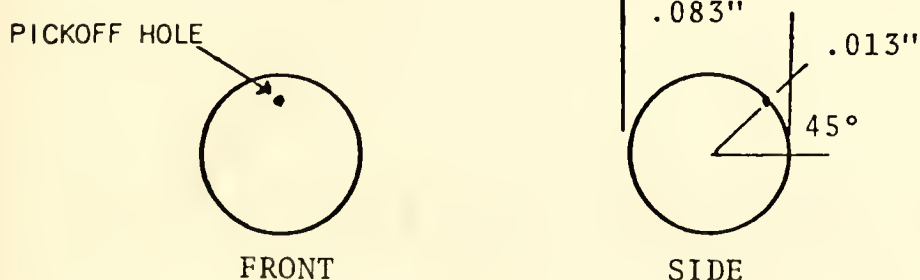
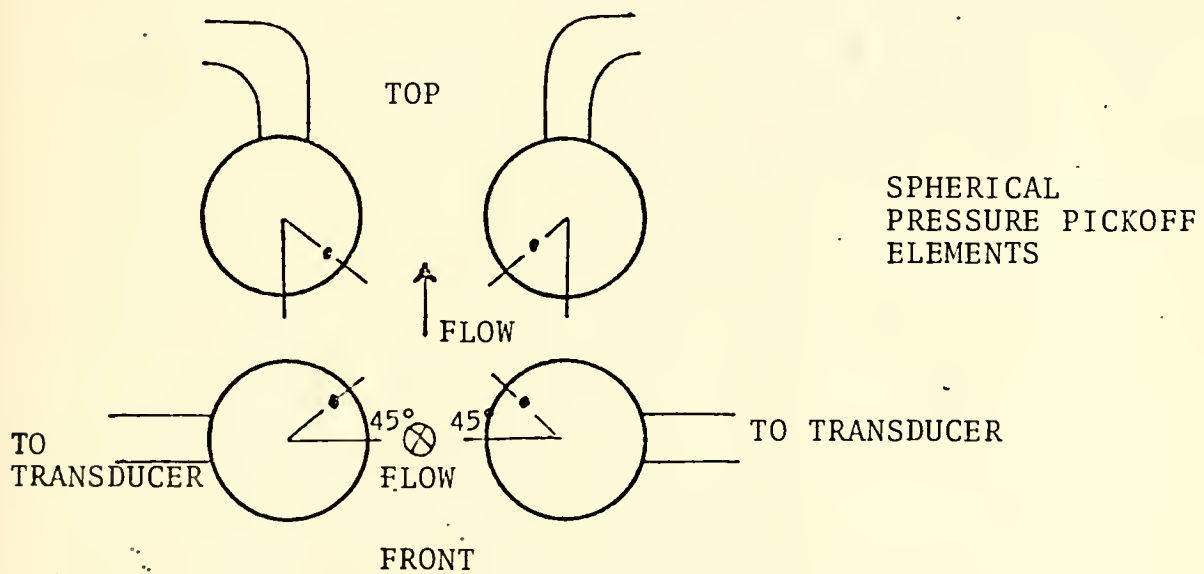
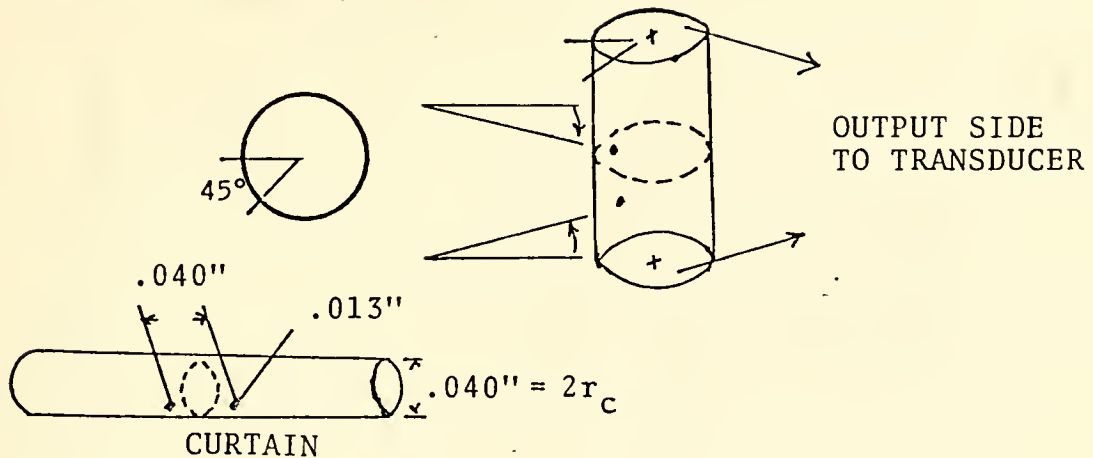


Figure 4. Pickoff Elements.

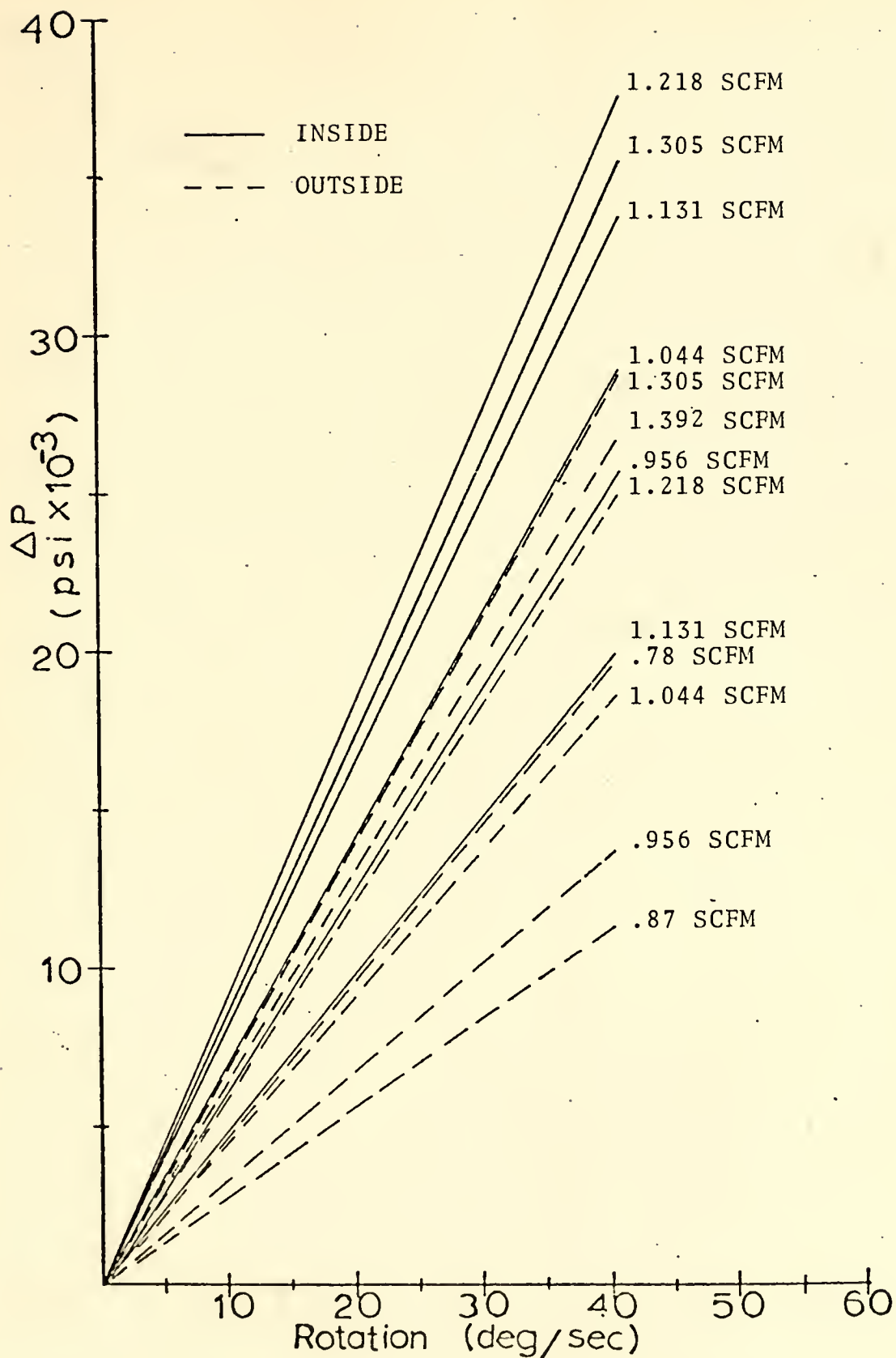


Figure 5. Differential Pressure vs. Angular Velocity (summary for spherical elements).

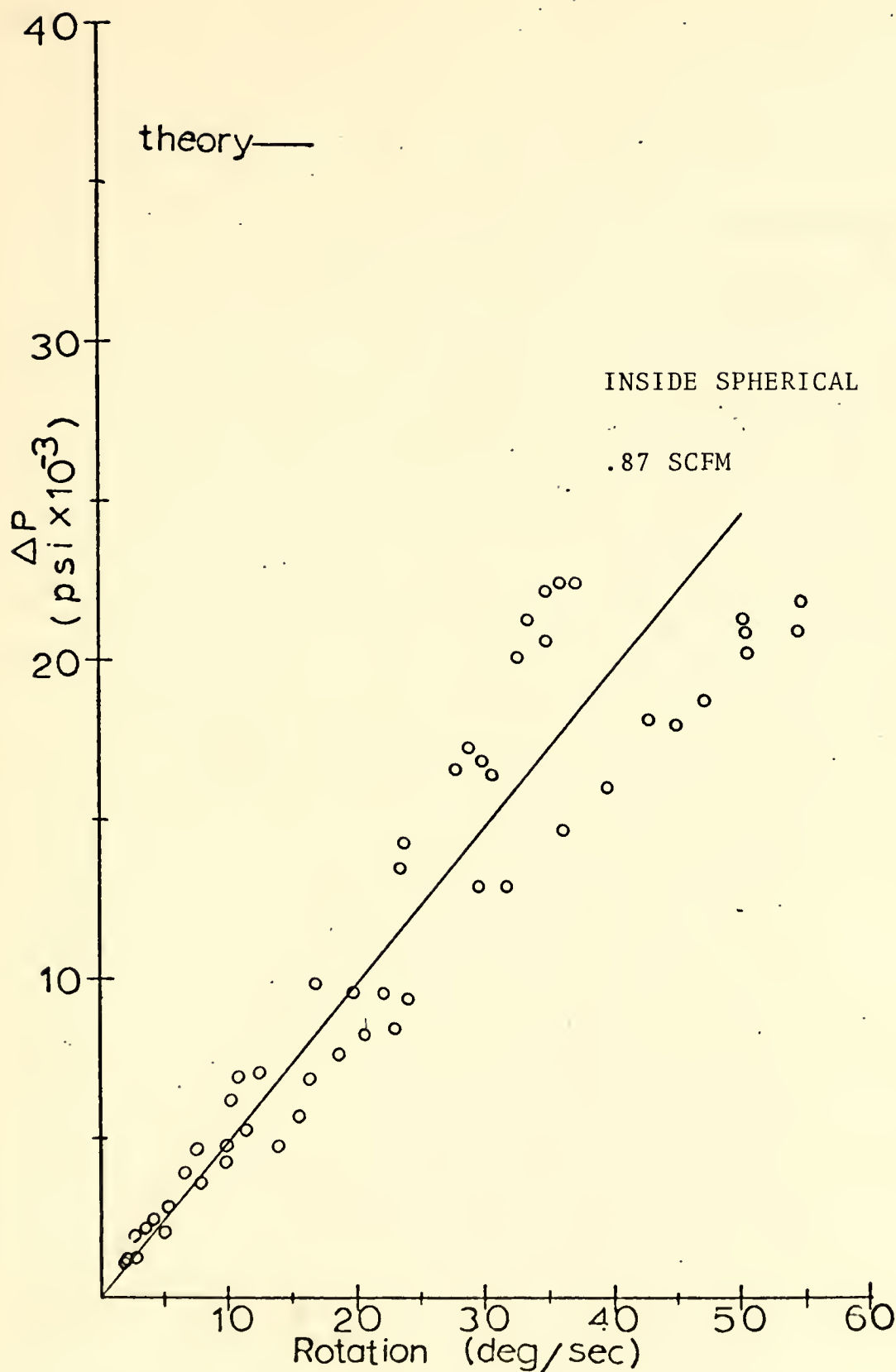


Figure 6. Differential Pressure vs. Angular Velocity (inserted spherical elements .87 SCFM).

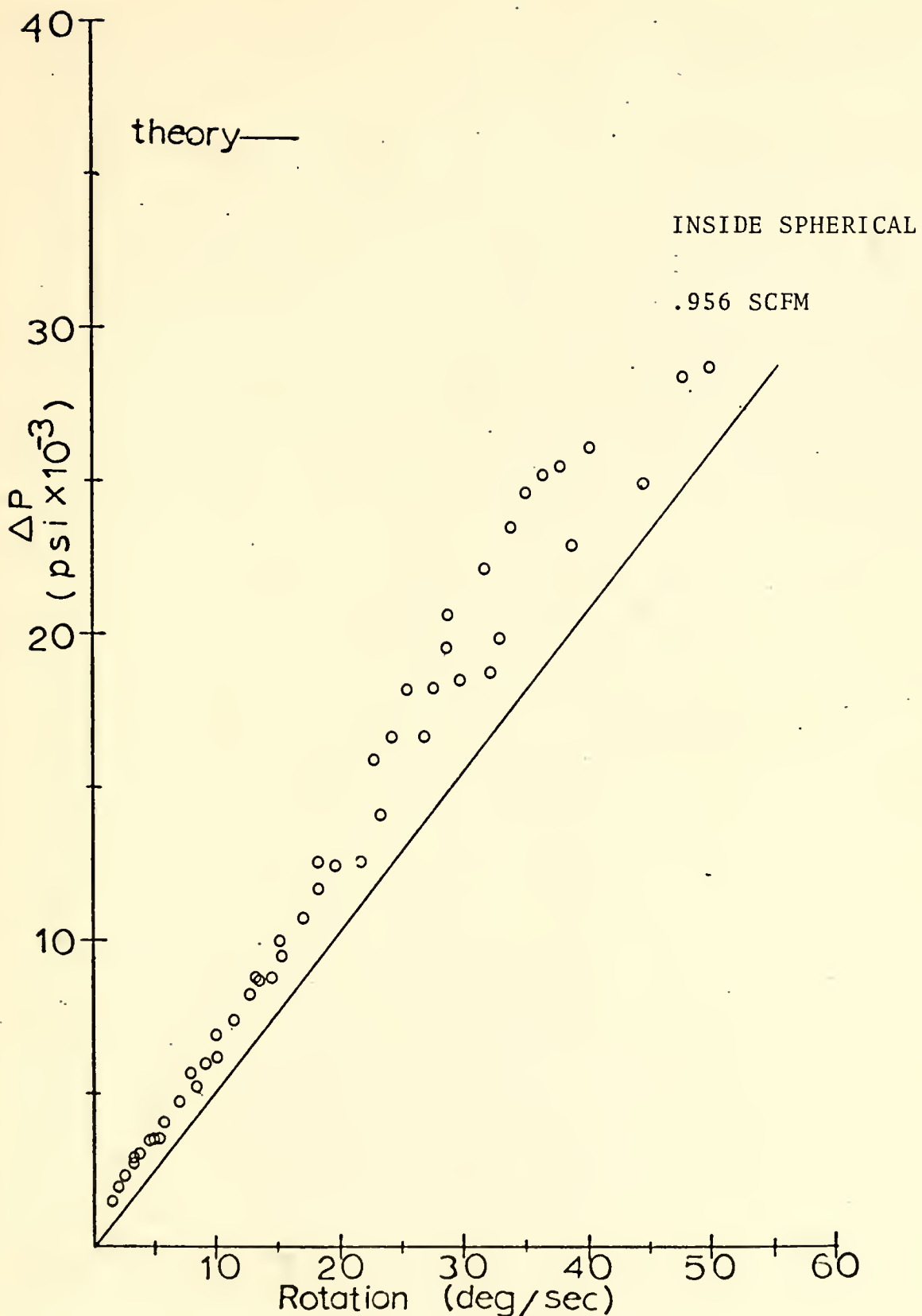


Figure 7. Differential Pressure vs. Angular Velocity (inserted spherical elements .956 SCFM).

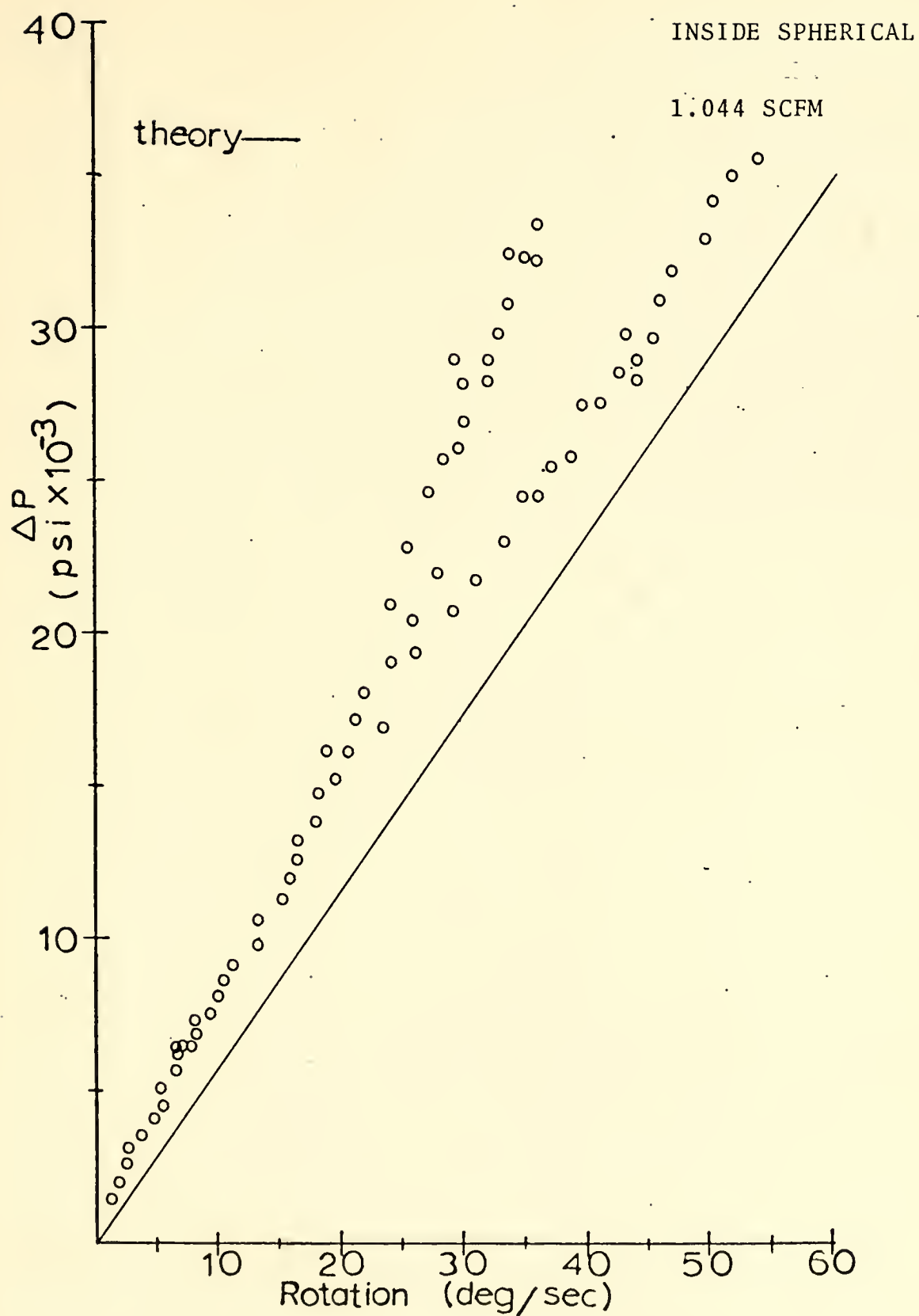


Figure 8. Differential Pressure vs. Angular Velocity (inserted spherical elements 1.044 SCFM).

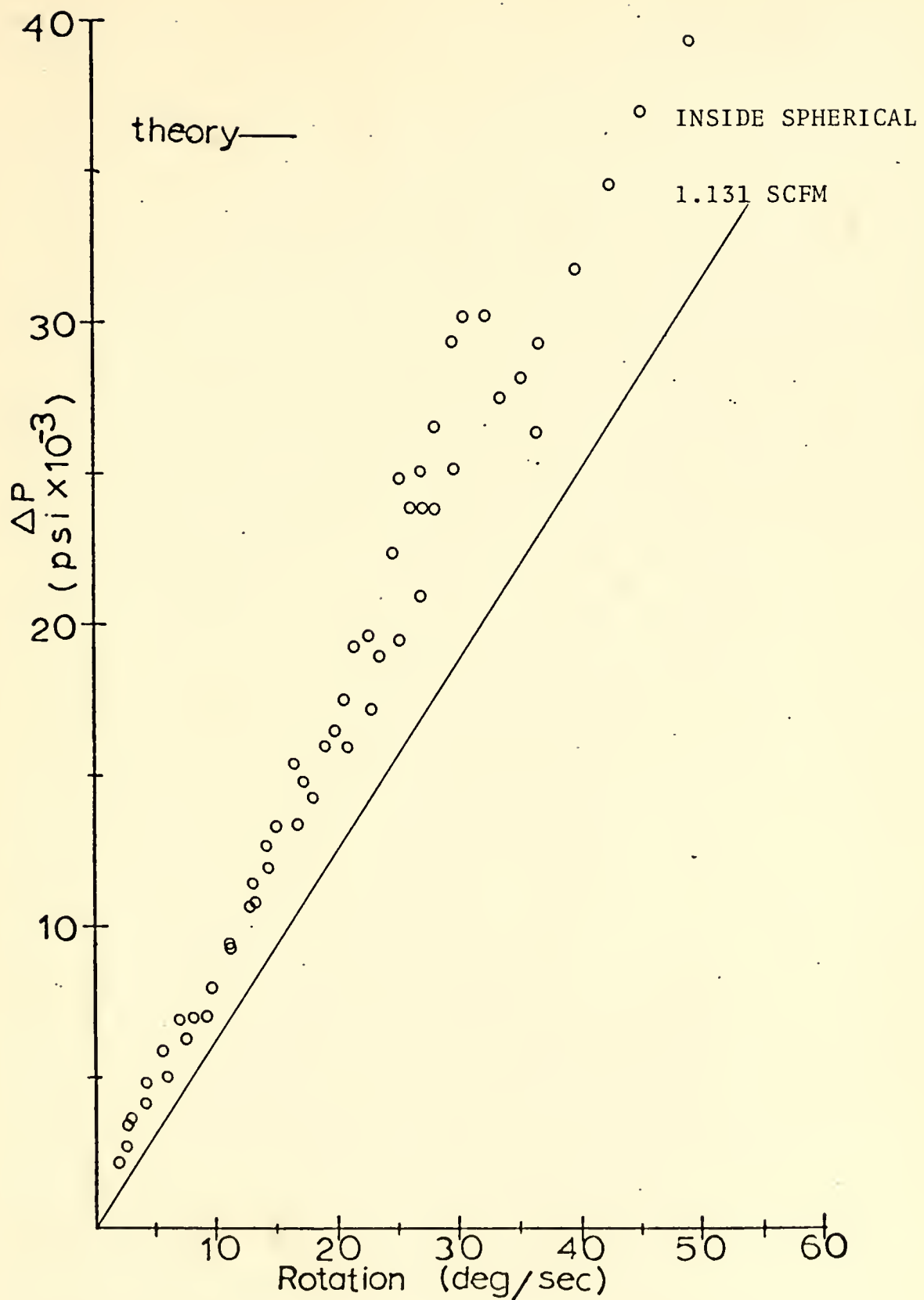


Figure 9. Differential Pressure vs. Angular Velocity (inserted spherical elements 1.131 SCFM).

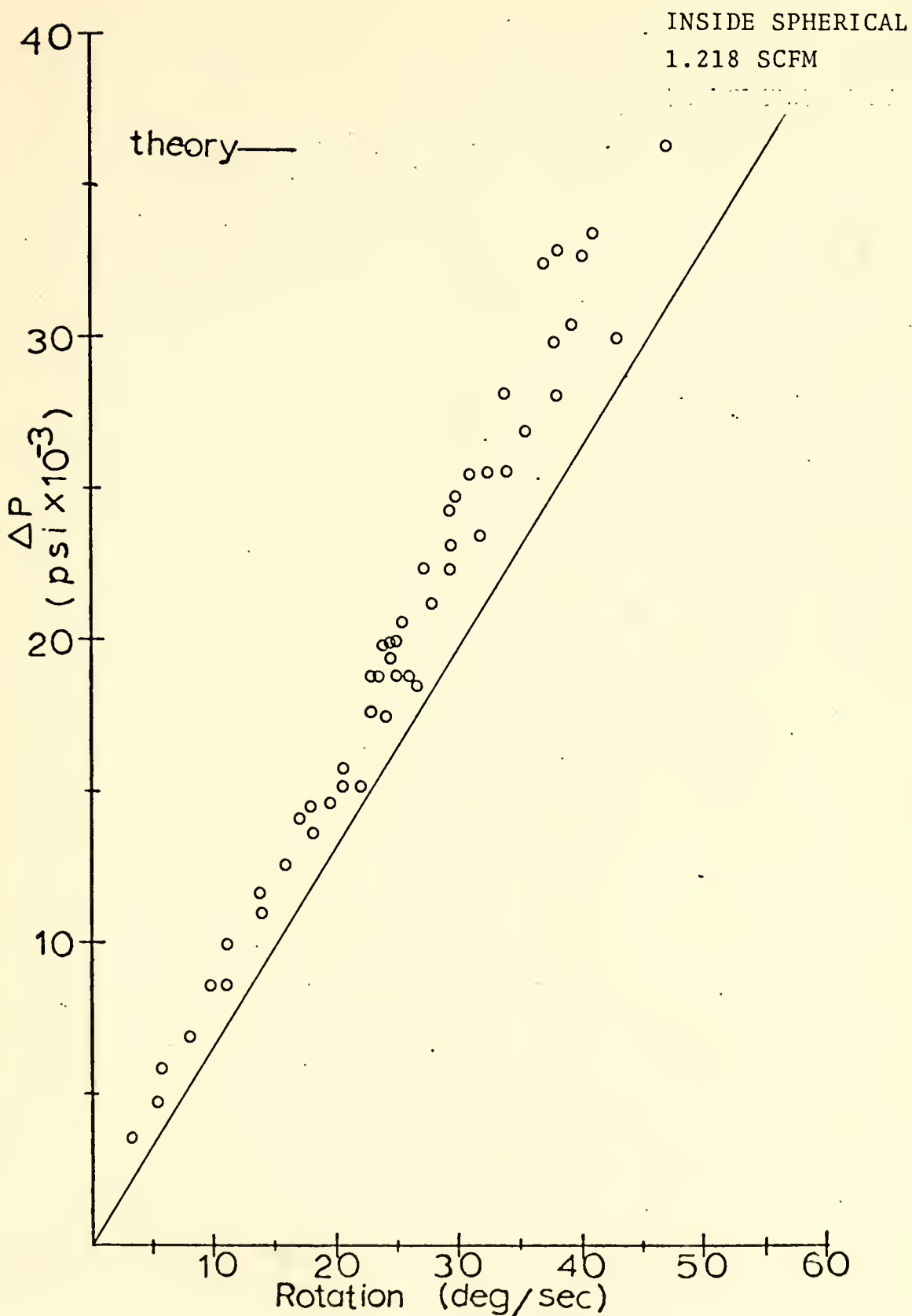


Figure 10. Differential Pressure vs. Angular Velocity
(inserted spherical elements 1.218 SCFM).

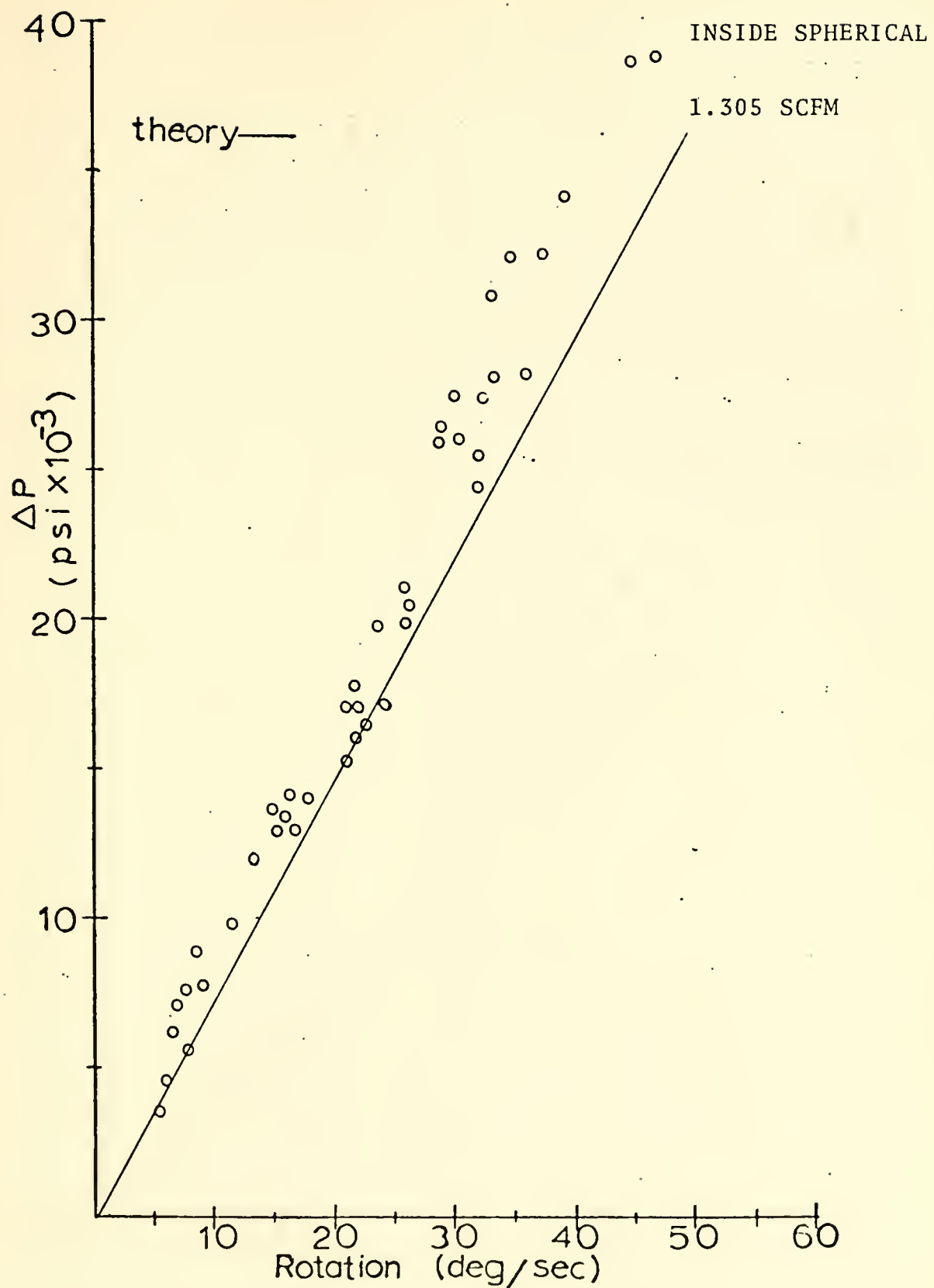


Figure 11. Differential Pressure vs. Angular Velocity (inserted spherical elements 1.305 SCFM).

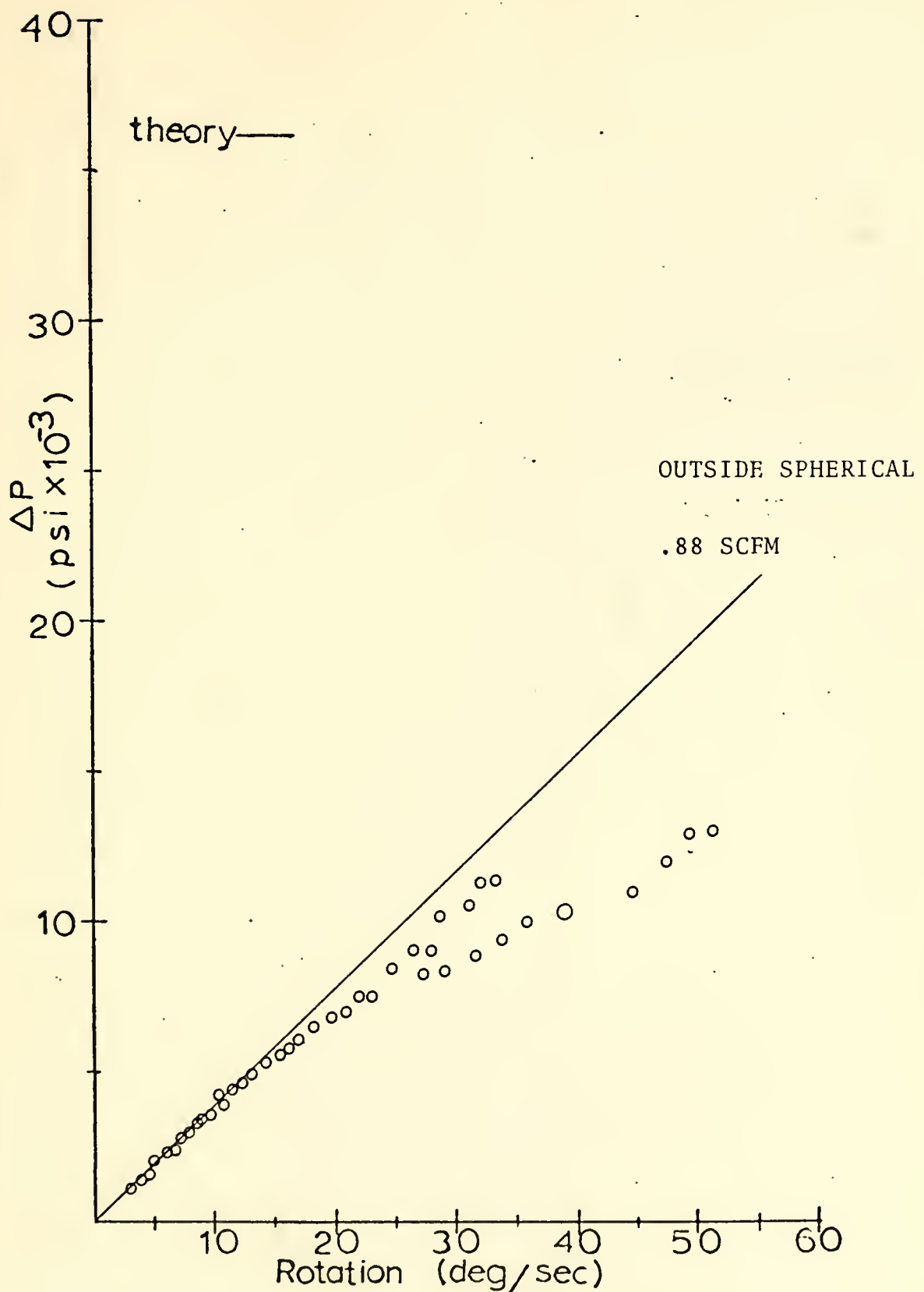


Figure 12. Differential Pressure vs. Angular Velocity (outside spherical elements .87 SCFM).

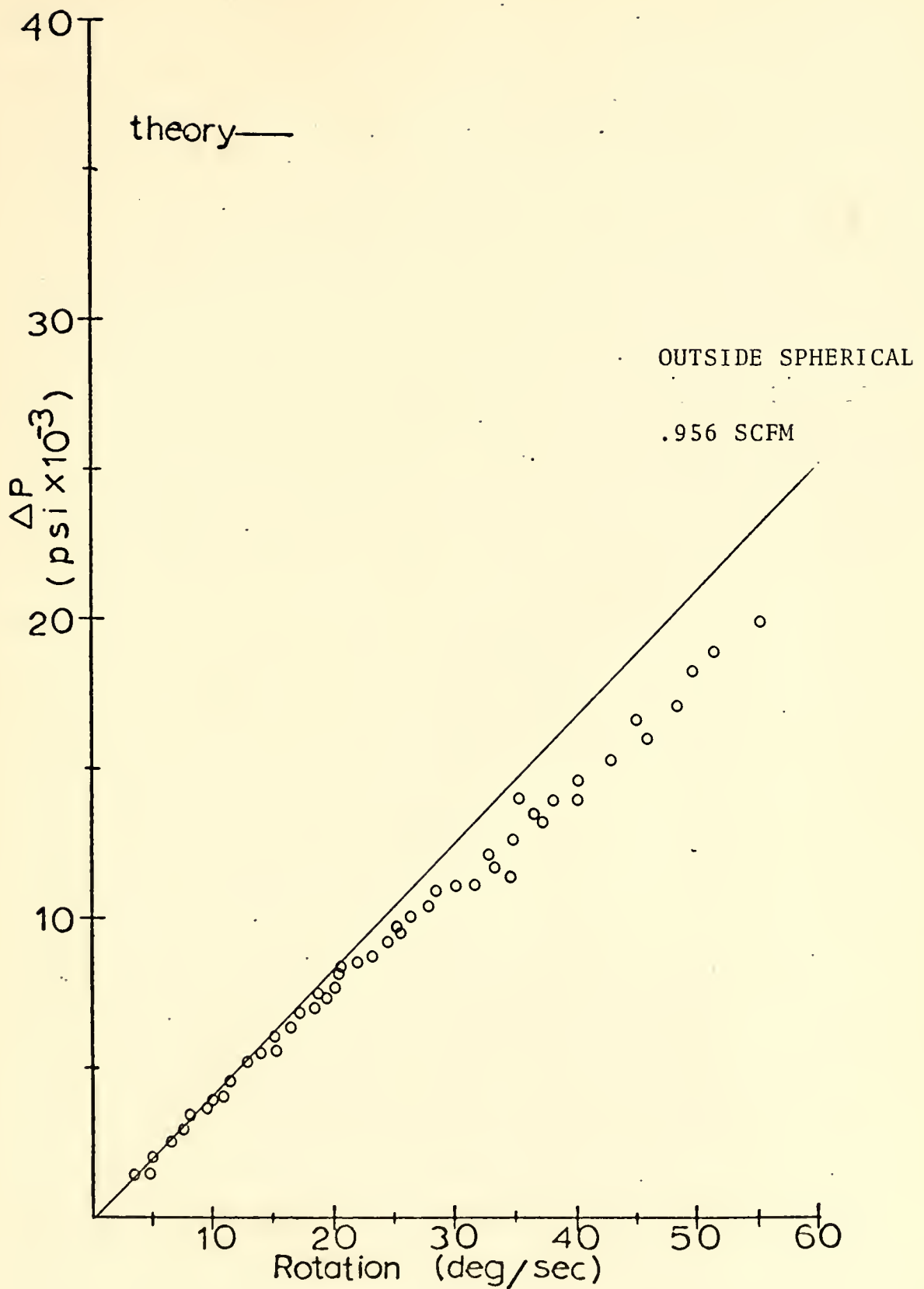


Figure 13. Differential Pressure vs. Angular Velocity (outside spherical elements .956 SCFM).

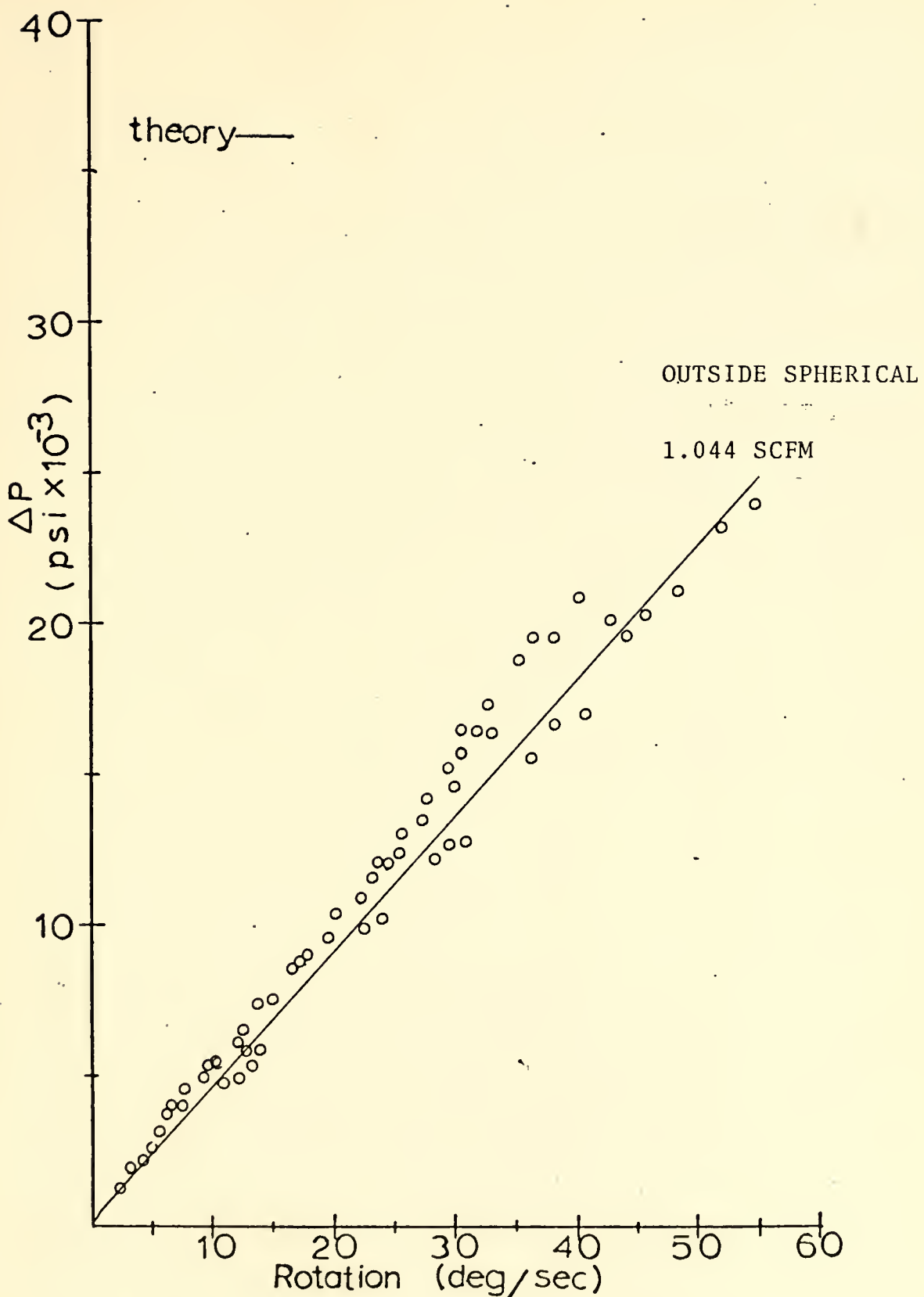


Figure 14. Differential Pressure vs. Angular Velocity (outside spherical elements 1.044 SCFM).

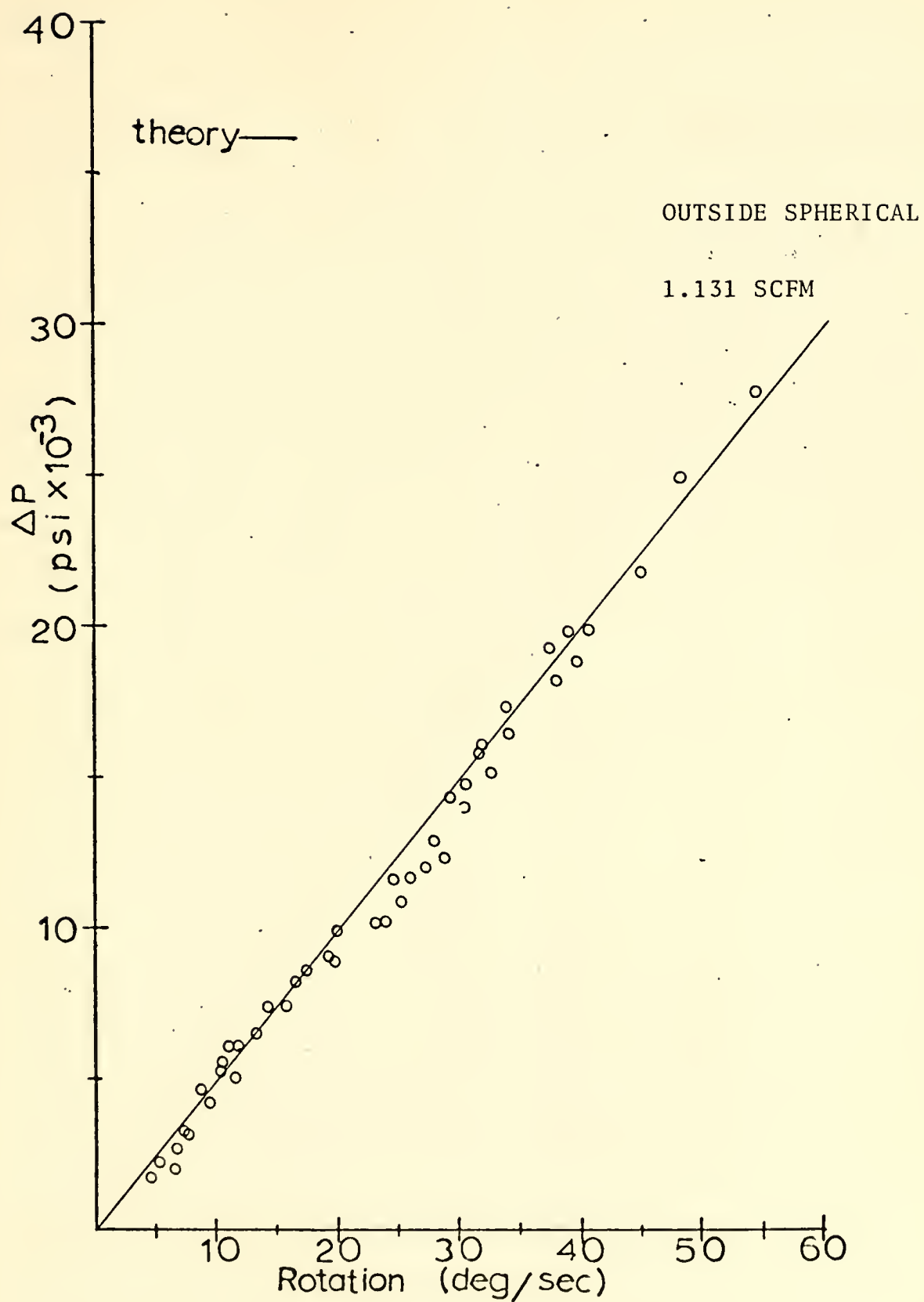


Figure 15. Differential Pressure vs. Angular Velocity (outside spherical elements 1.131 SCFM).

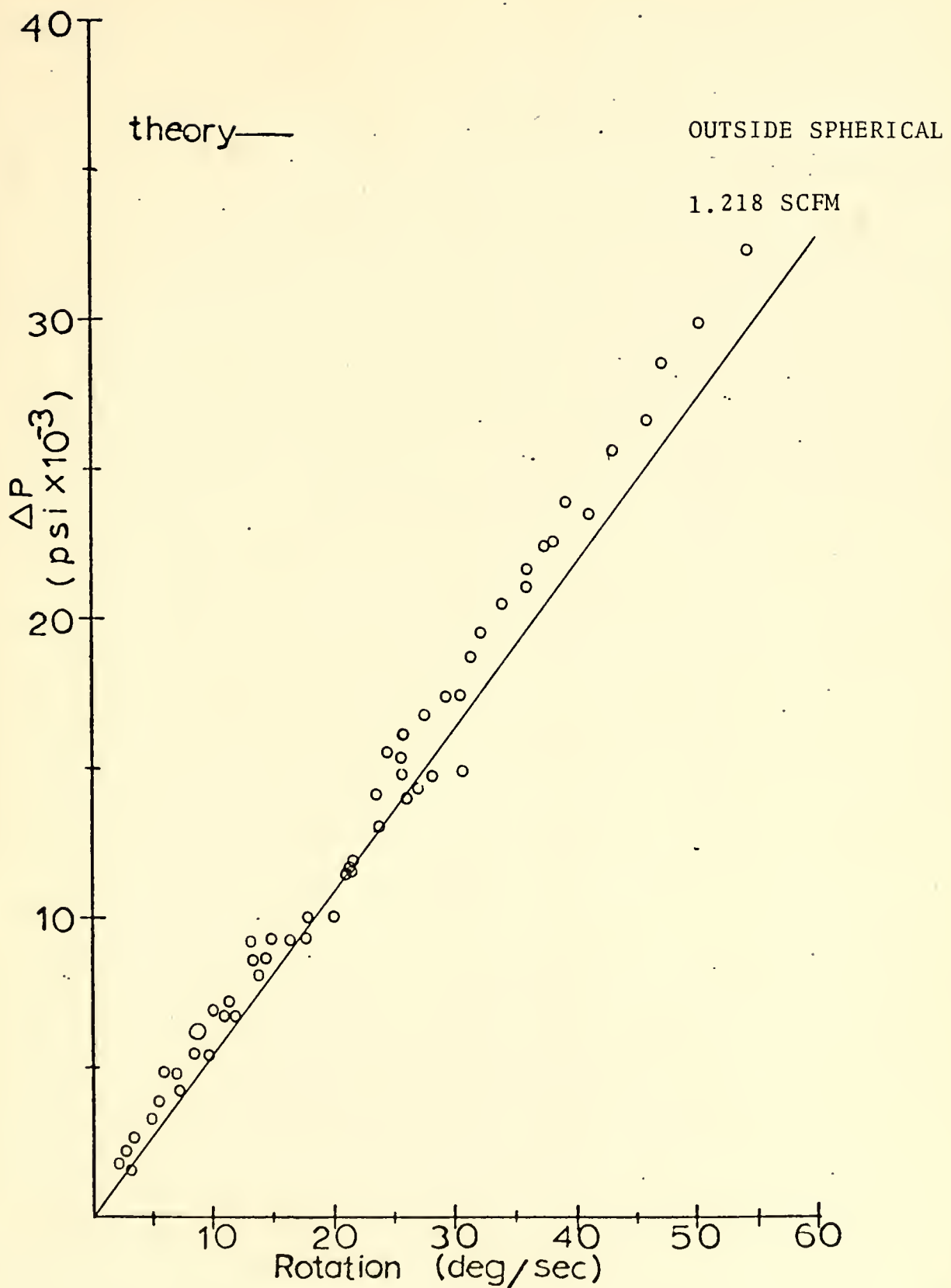


Figure 16. Differential Pressure vs. Angular Velocity (outside spherical elements 1.218 SCFM).

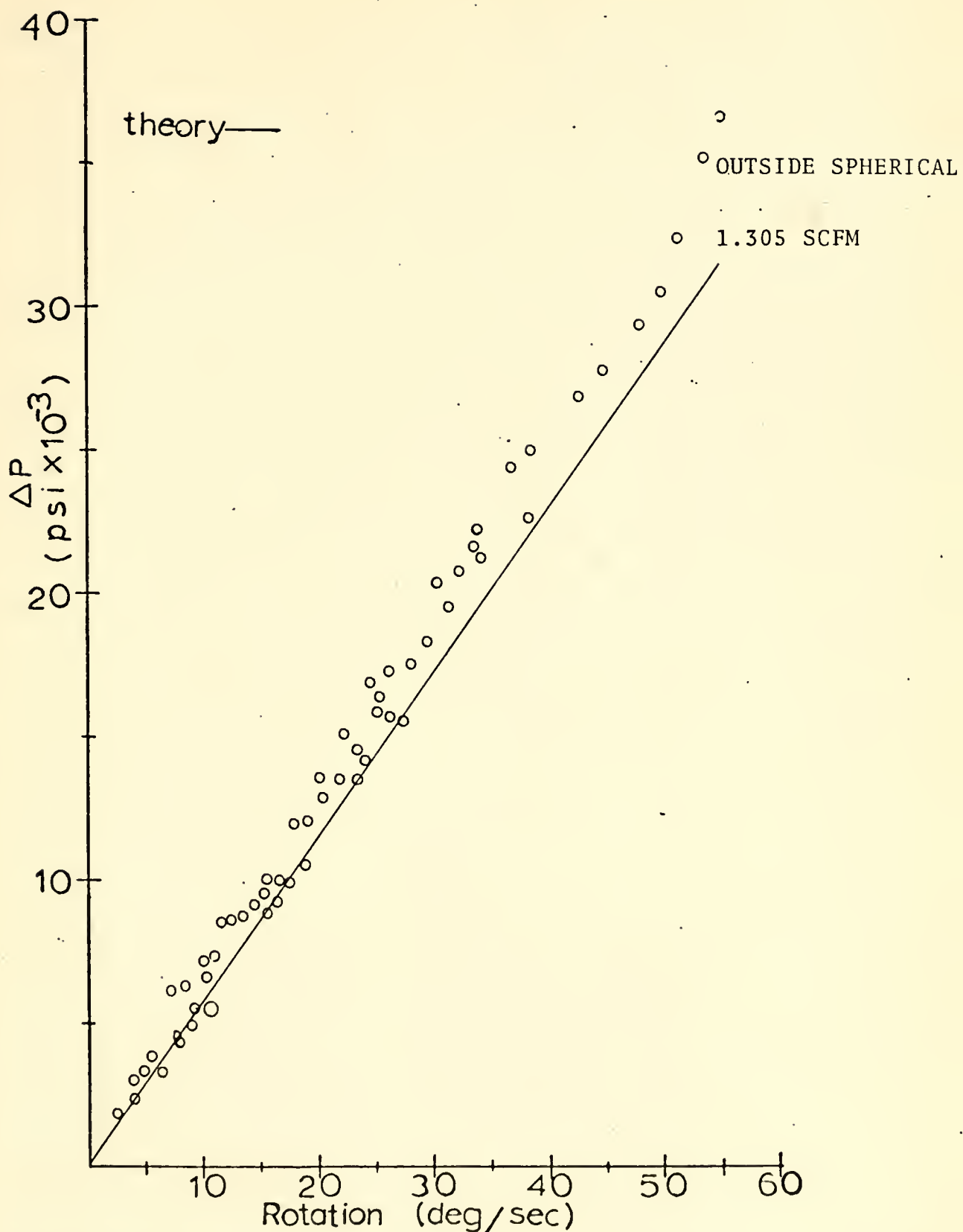


Figure 17. Differential Pressure vs. Angular Velocity (outside spherical elements 1.305 SCFM).

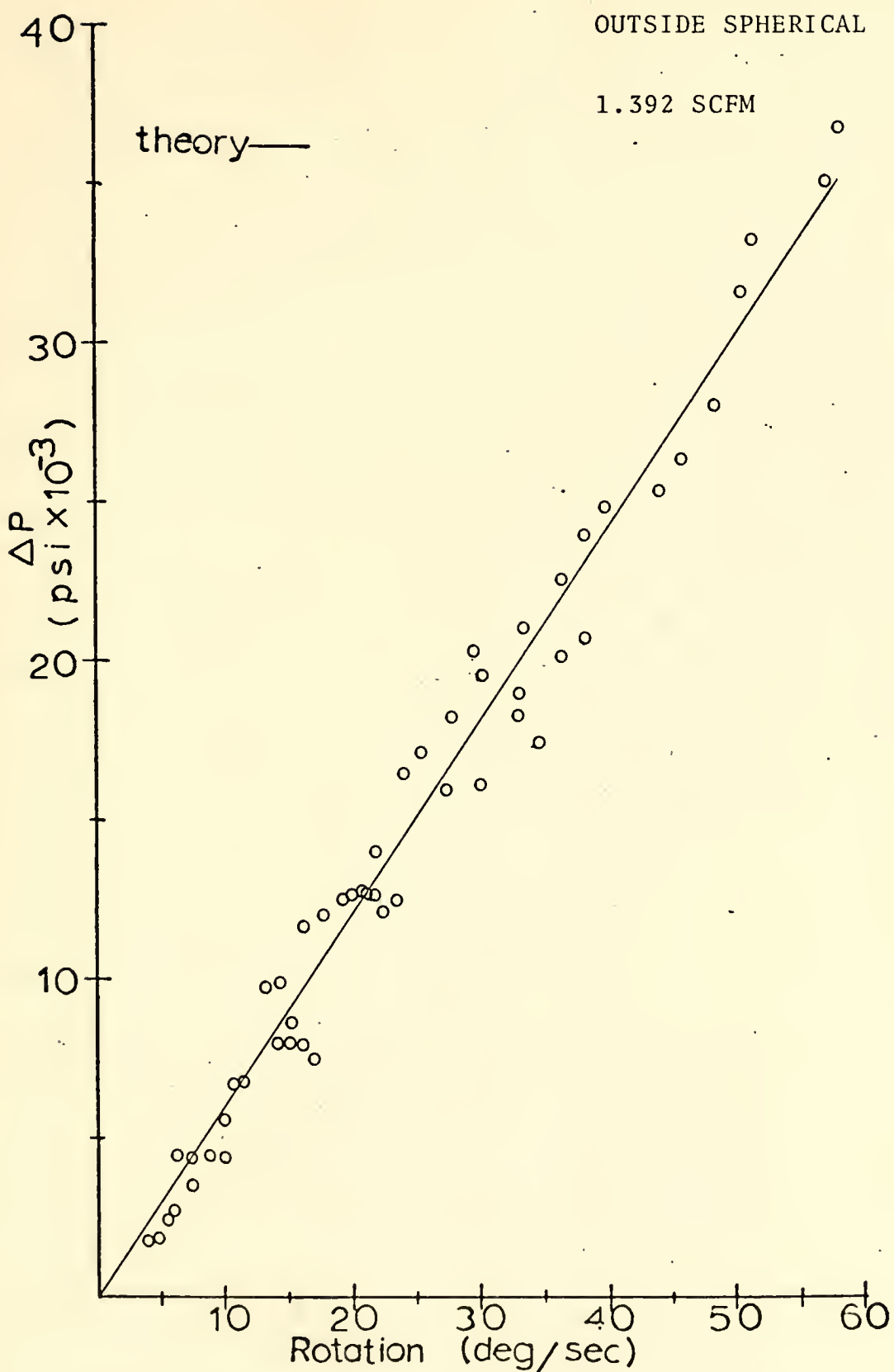


Figure 18. Differential Pressure vs. Angular Velocity (outside spherical elements 1.392 SCFM).

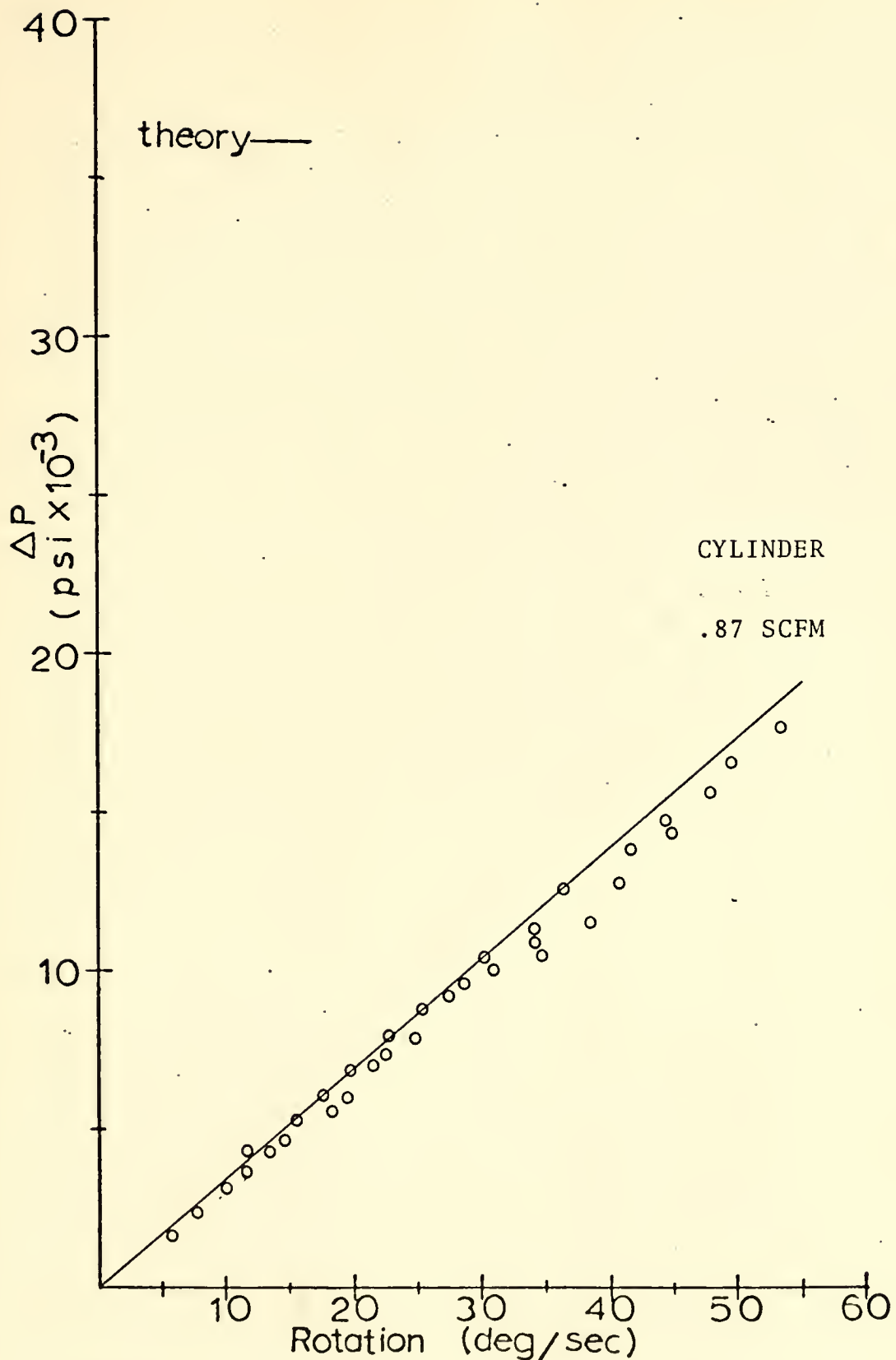


Figure 19. Differential Pressure vs. Angular Velocity (cylindrical element .87 SCFM).

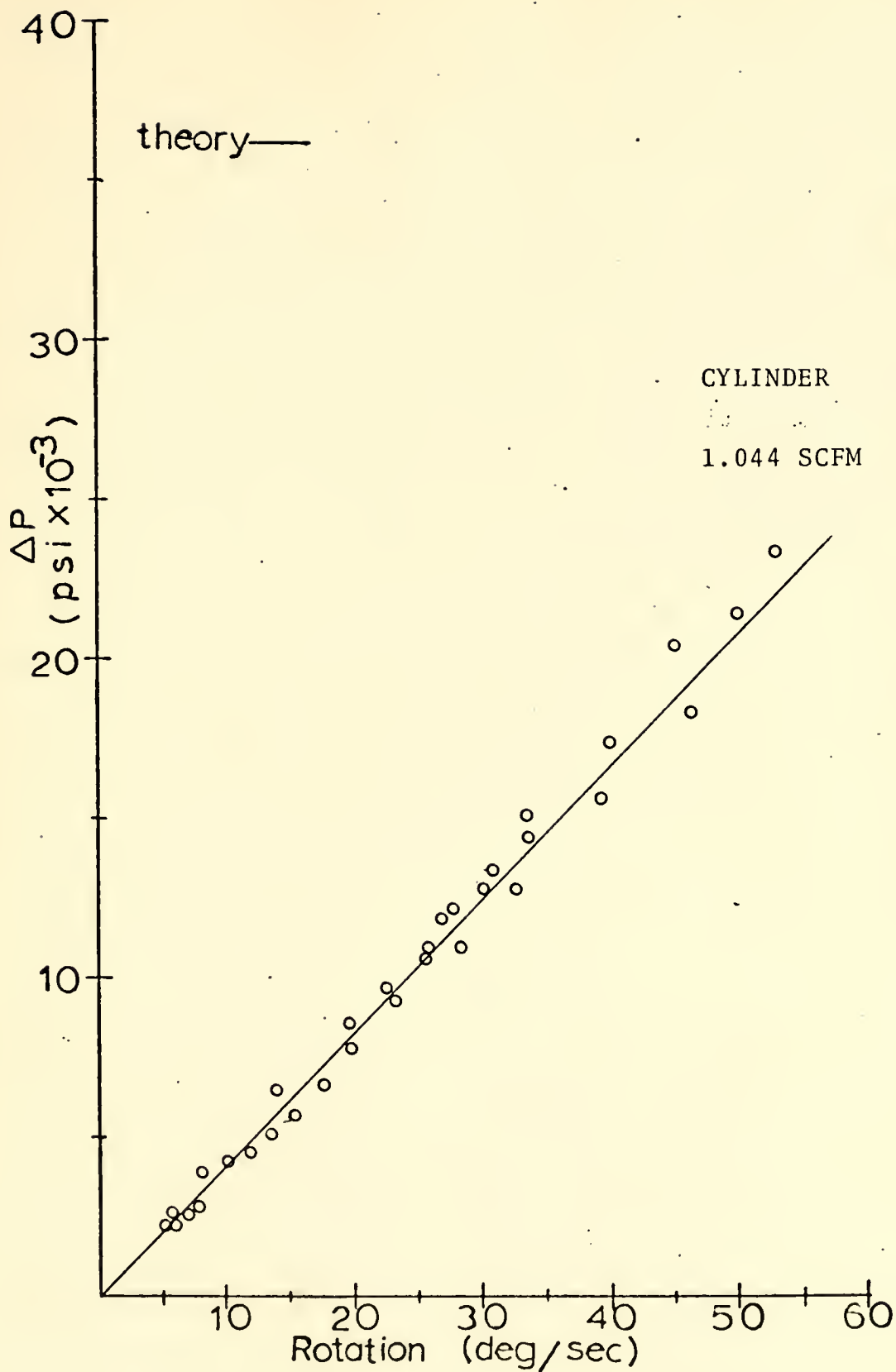


Figure 20. Differential Pressure vs. Angular Velocity (cylindrical element 1.044 SCFM).

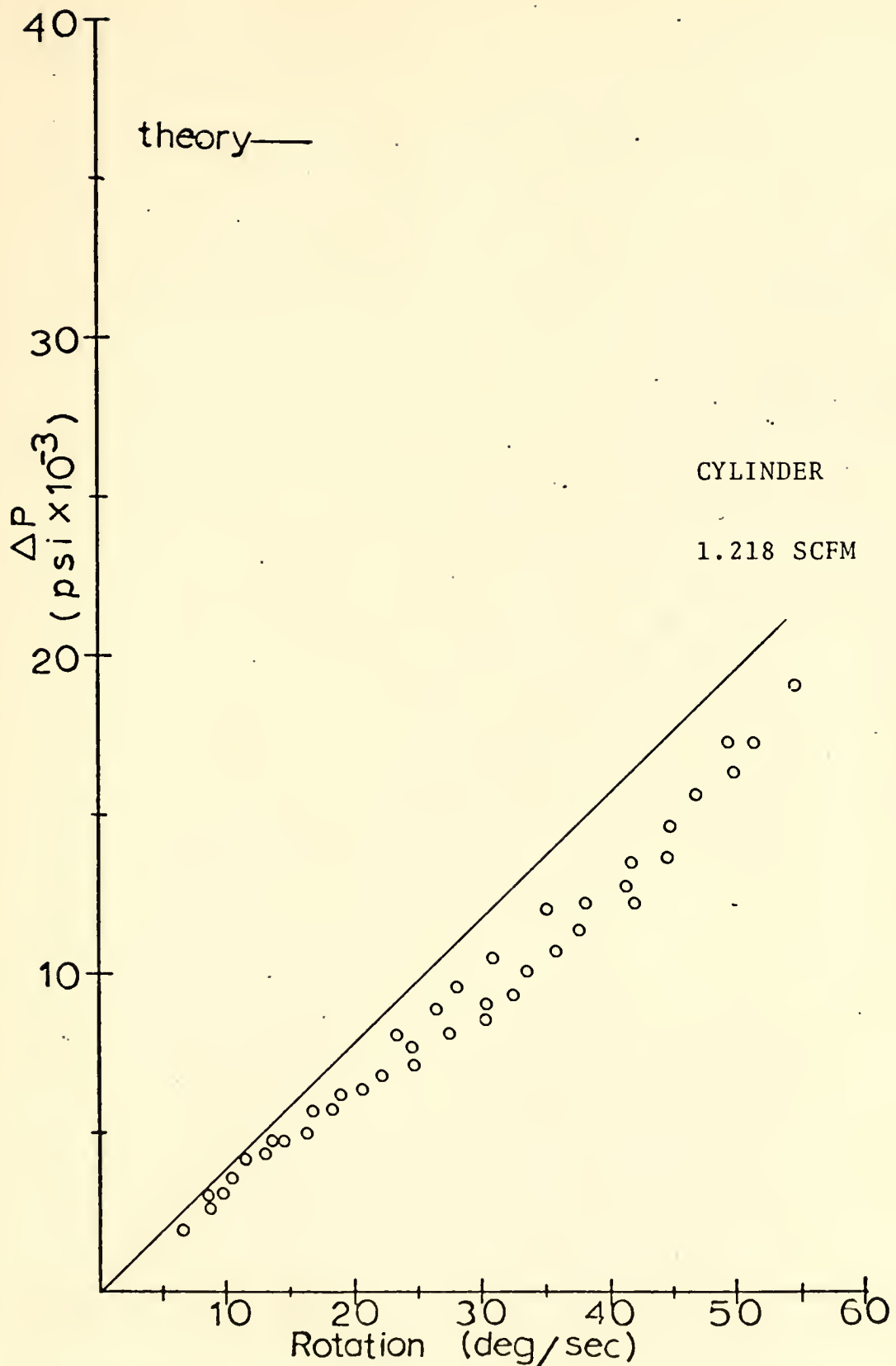


Figure 21. Differential Pressure vs. Angular Velocity (cylindrical element 1.218 SCFM).

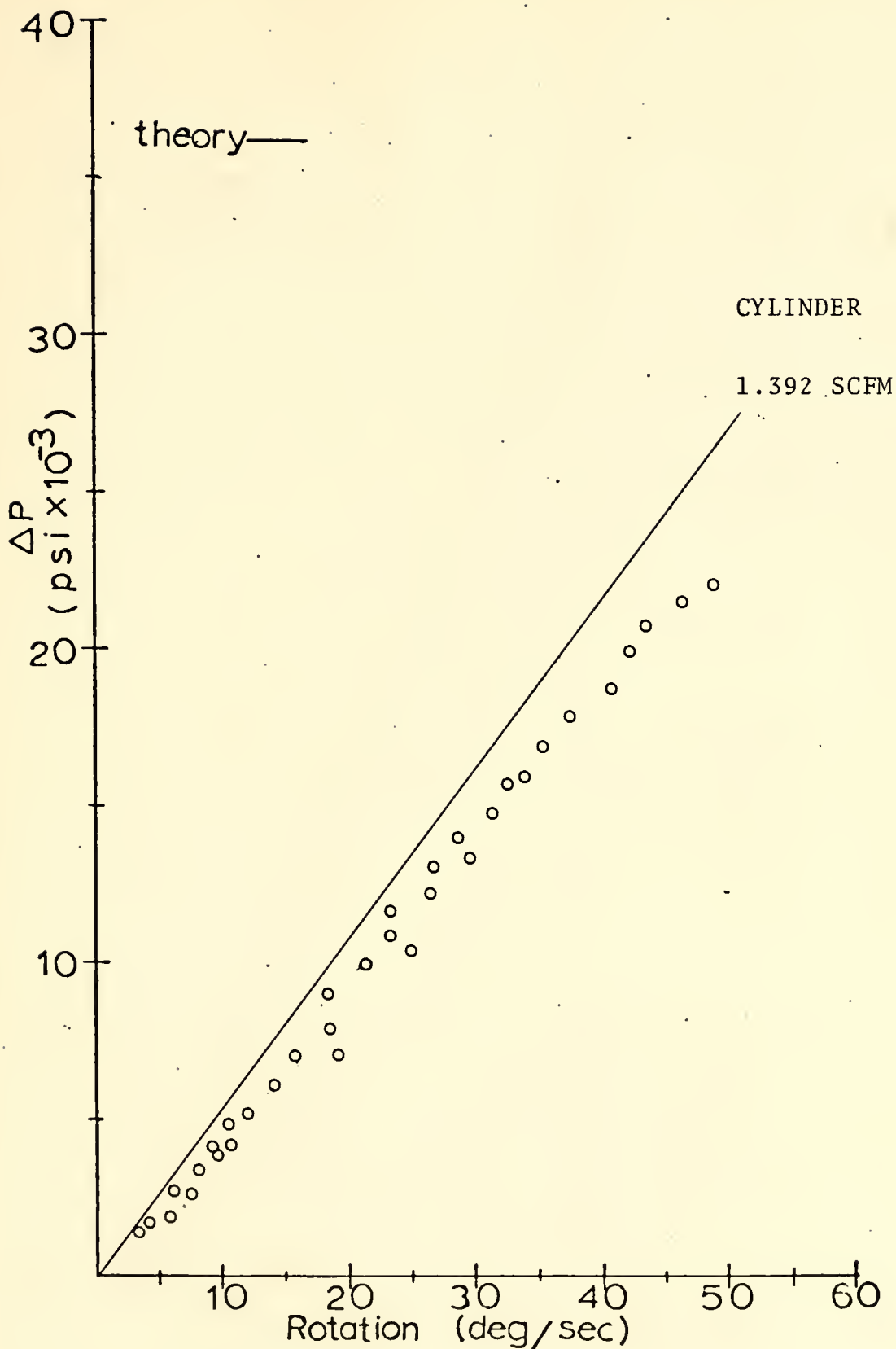


Figure 22. Differential Pressure vs. Angular Velocity (cylindrical element 1.392 SCFM).

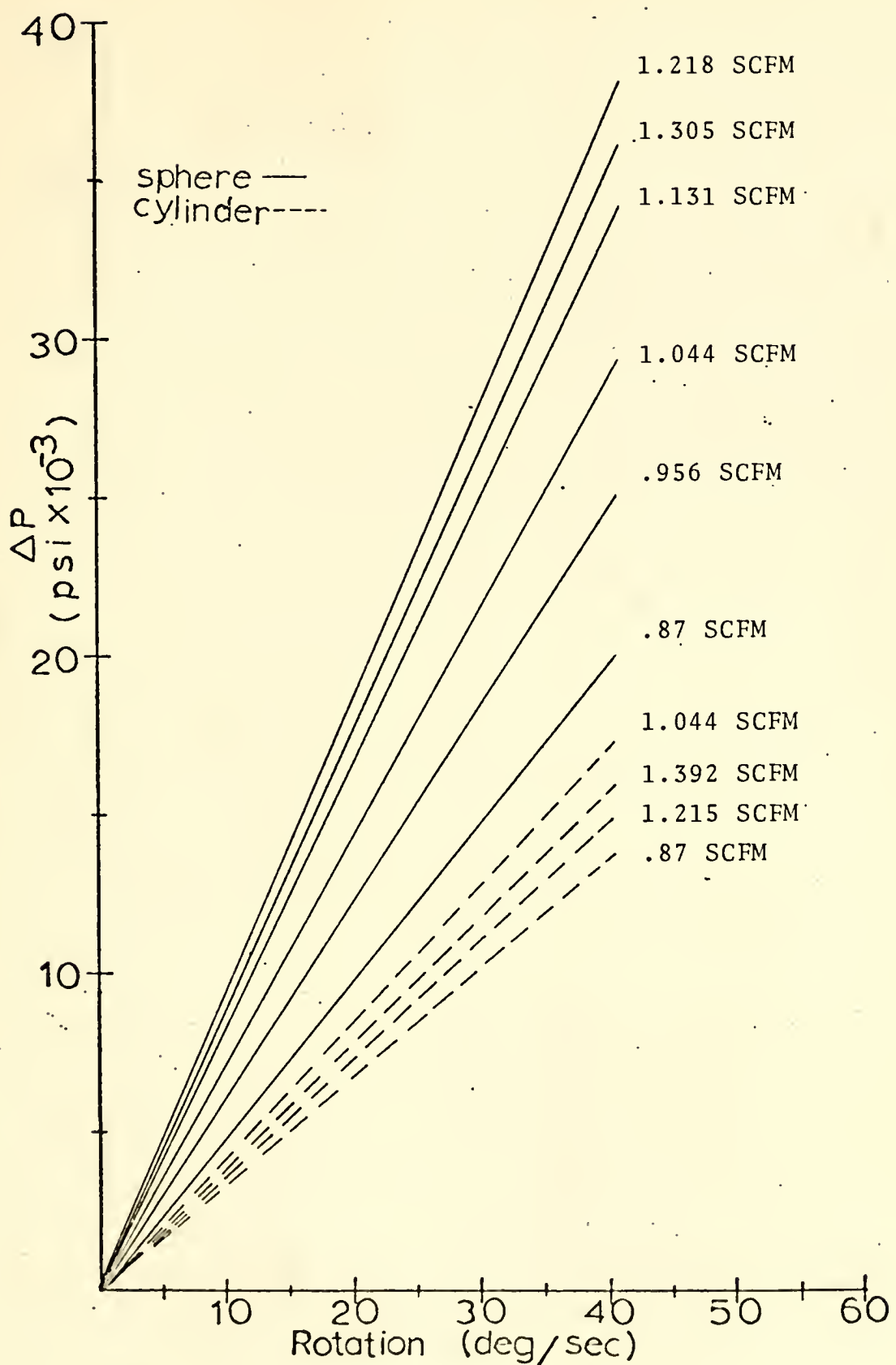


Figure 23. Differential Pressure vs. Angular Velocity (spherical cylindrical comparison).

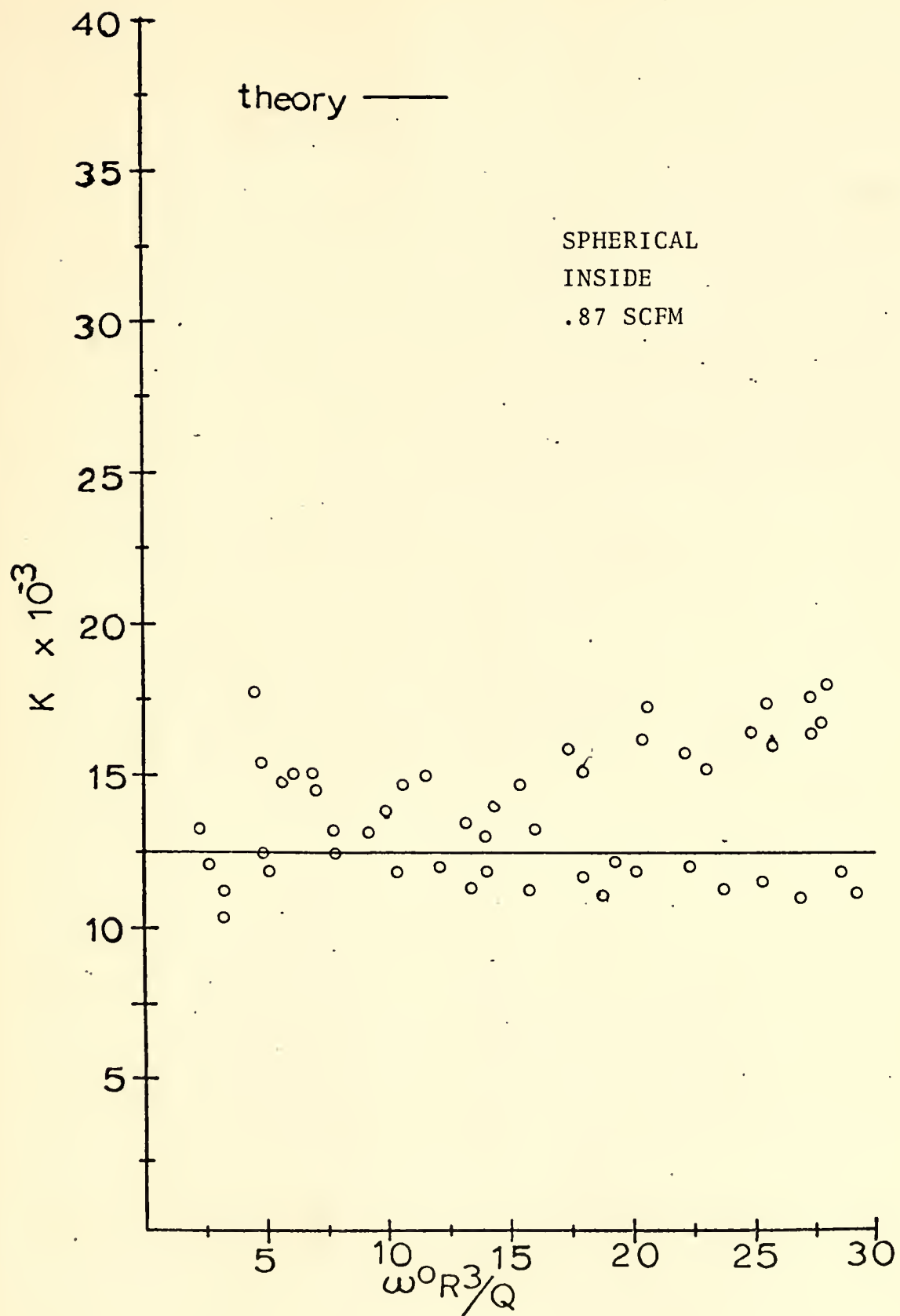


Figure 24. K vs. $\omega^0 R^3 / Q$ (inserted spherical elements .87 SCFM).

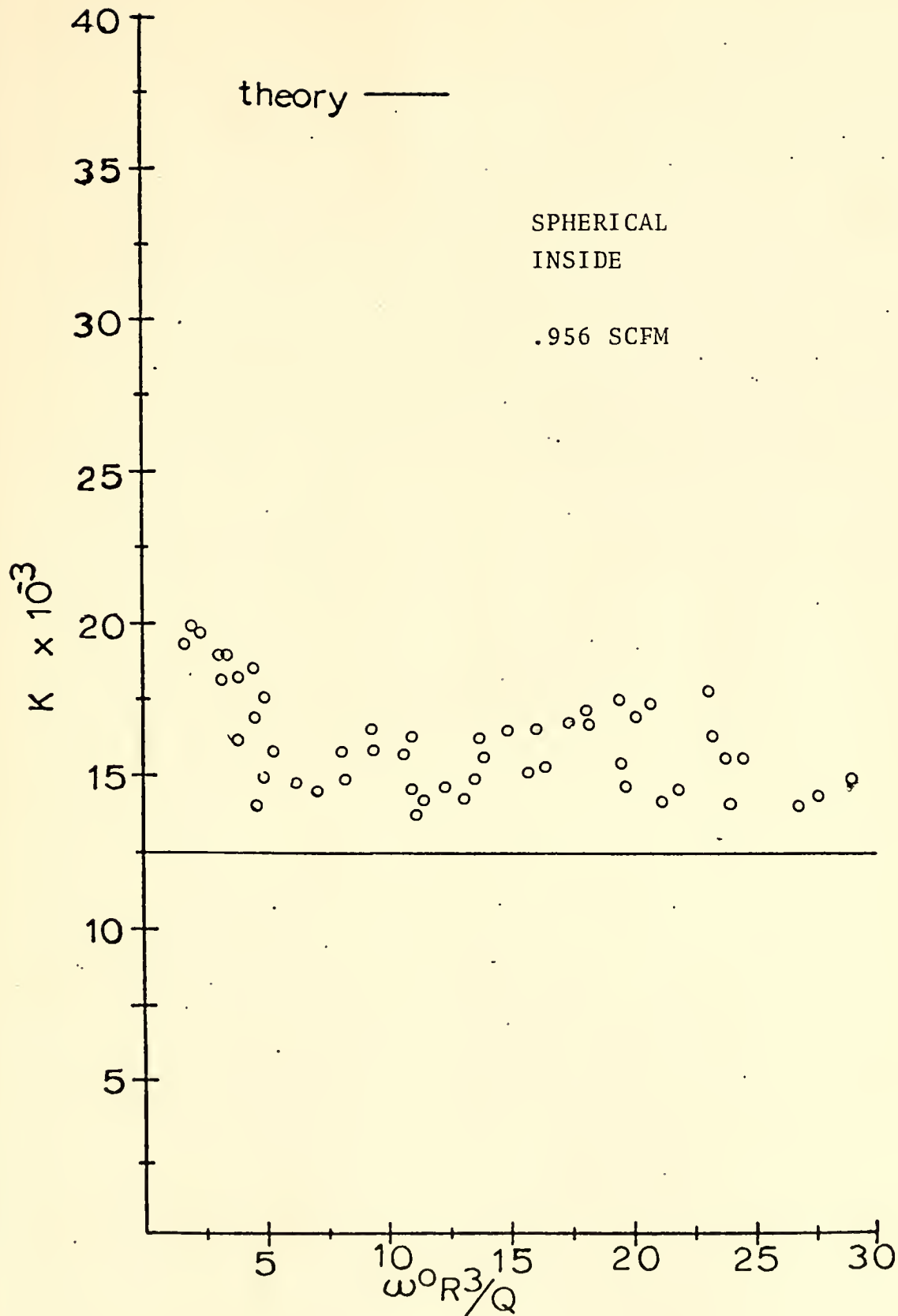


Figure 25. K vs. $\omega^0 R^3 / Q$ (inserted spherical elements .956 SCFM).

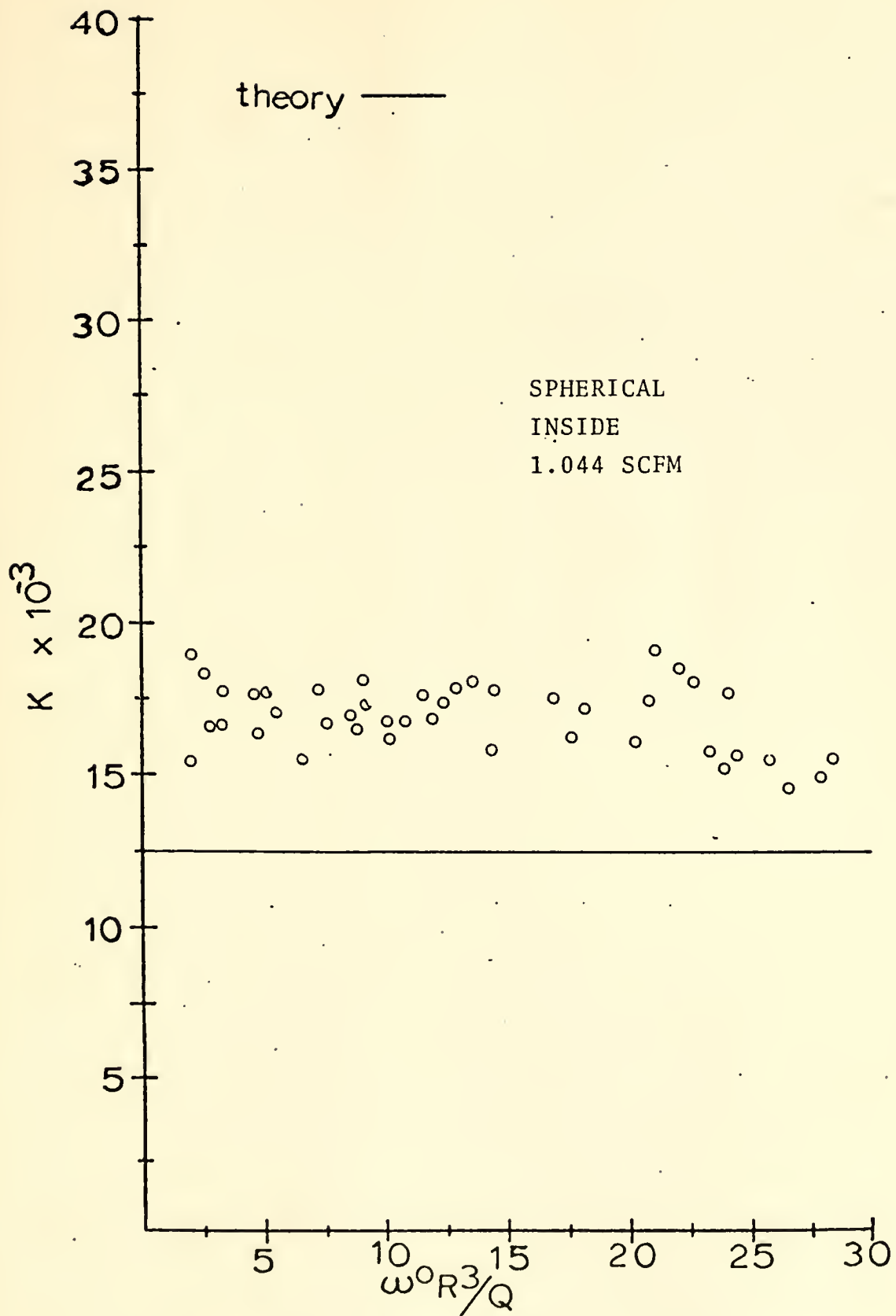


Figure 26. K vs. $\omega^0 R^3 / Q$ (inserted spherical elements 1.044 SCFM).

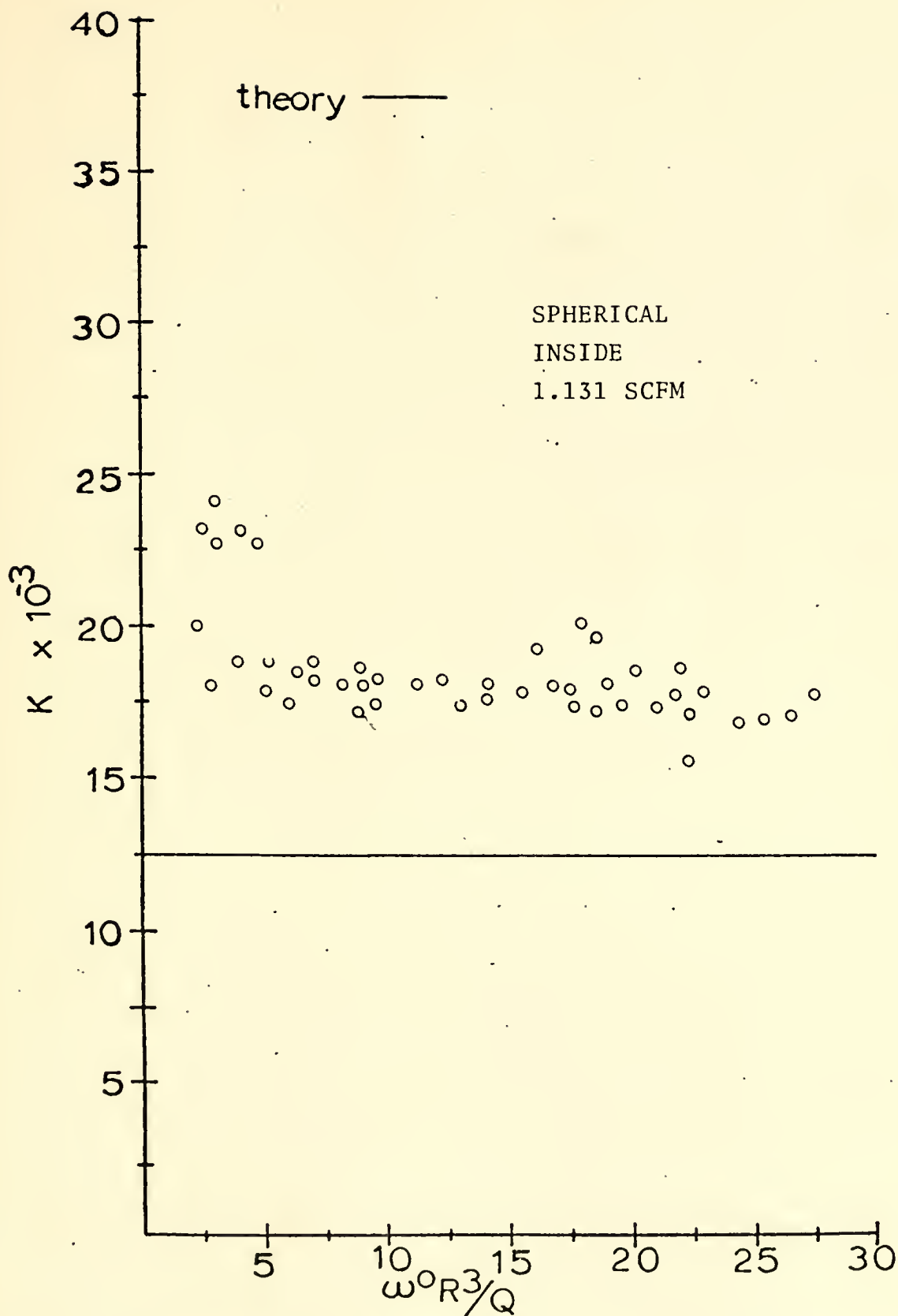


Figure 27. K vs. $\omega^0 R^3 / Q$ (inserted spherical elements 1.131 SCFM).

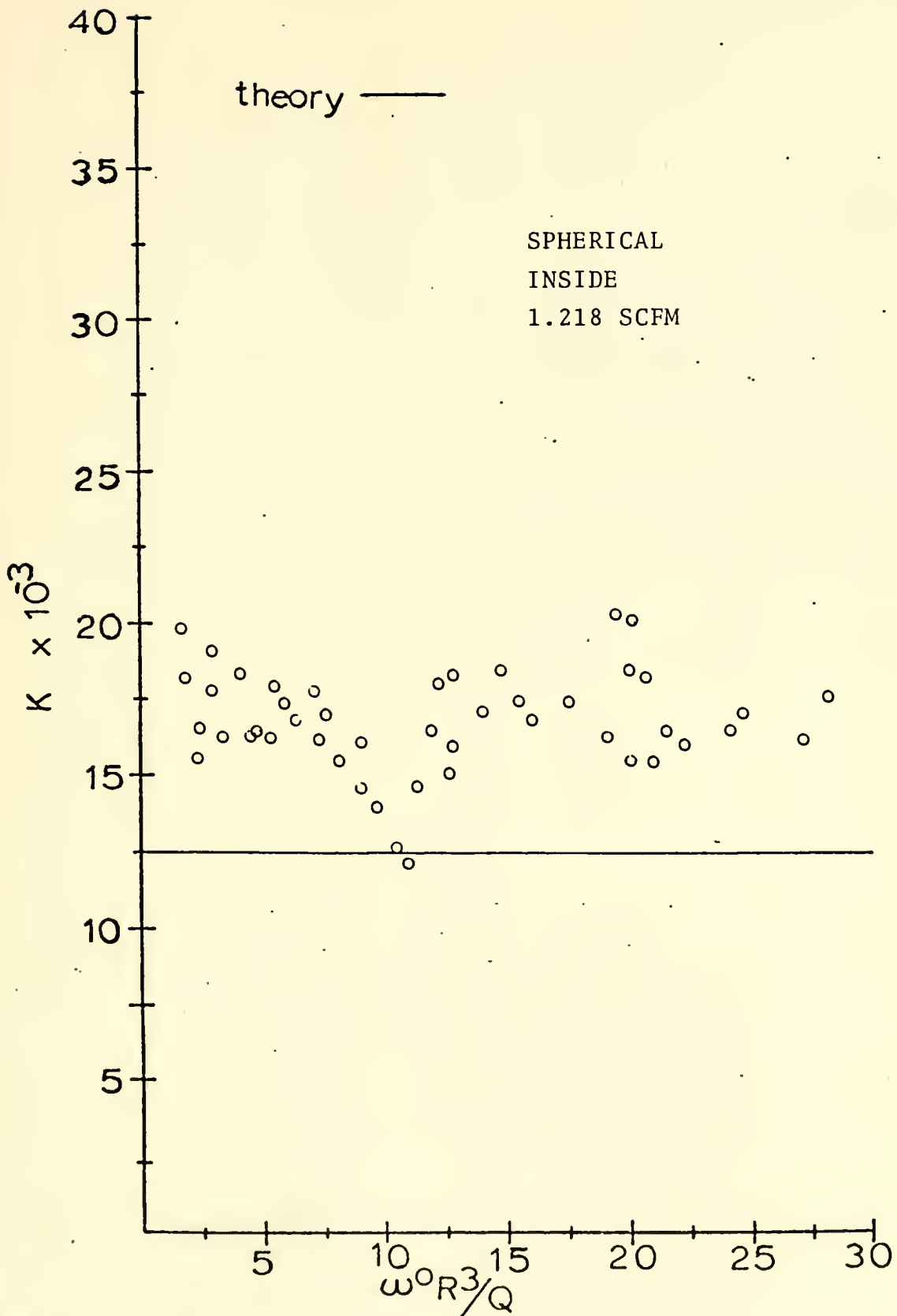


Figure 28. K vs. $\omega^0 R^3 / Q$ (inserted spherical elements 1.218 SCFM).

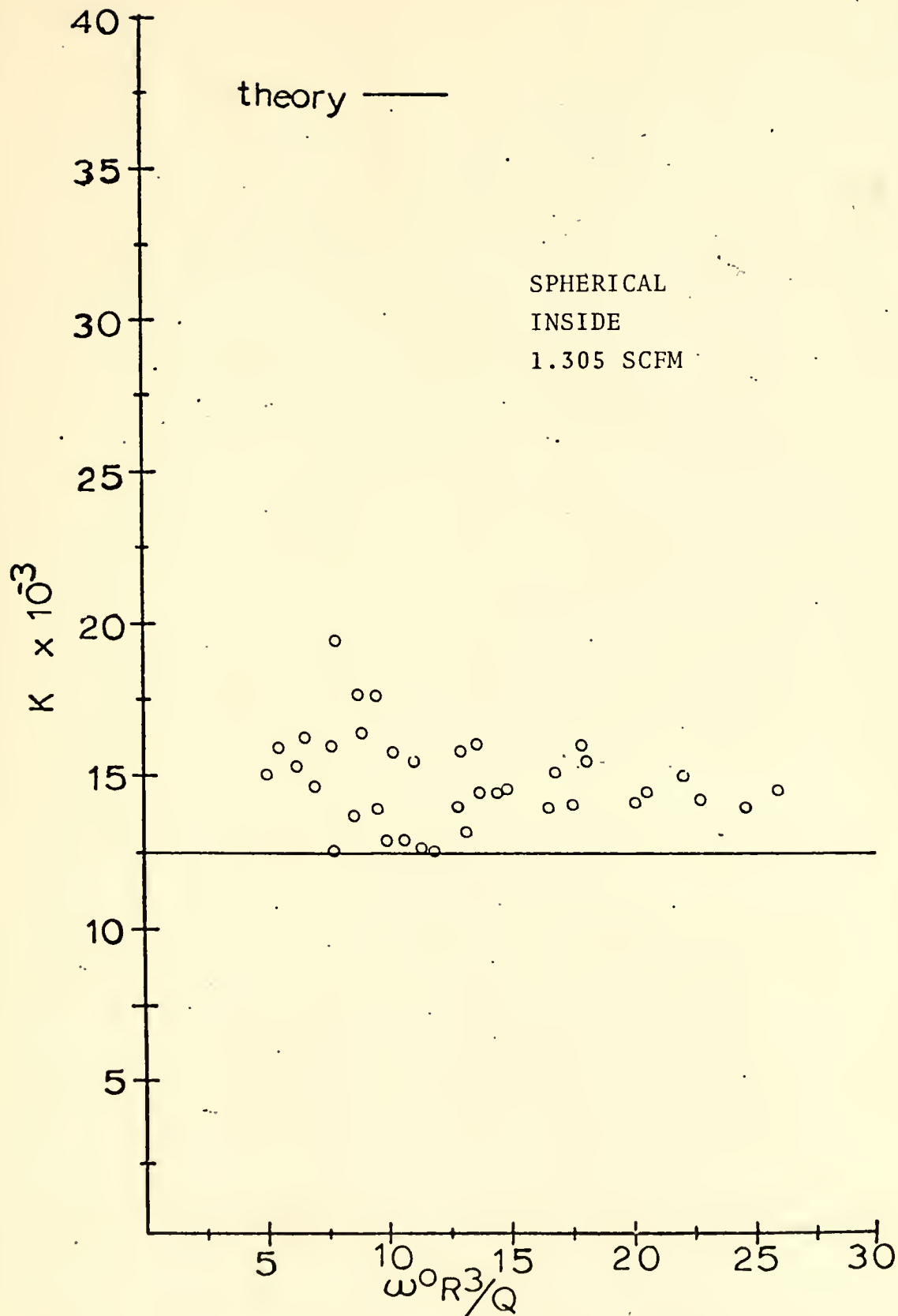


Figure 29. K vs. $\omega^0 R^3 / Q$ (inserted spherical elements 1.305 SCFM).

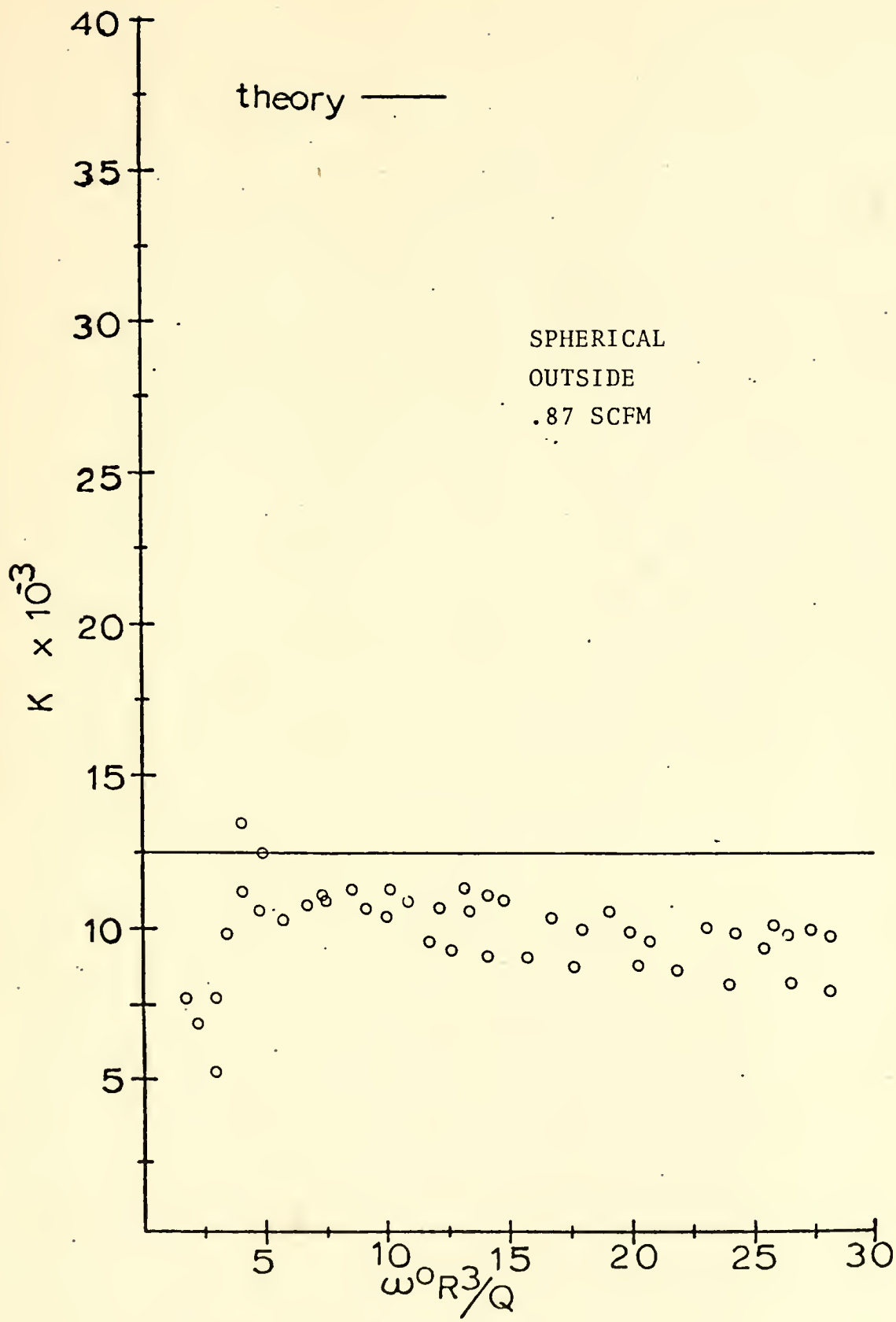


Figure 30. K vs. $\omega^0 R^3 / Q$ (outside spherical elements .87 SCFM).

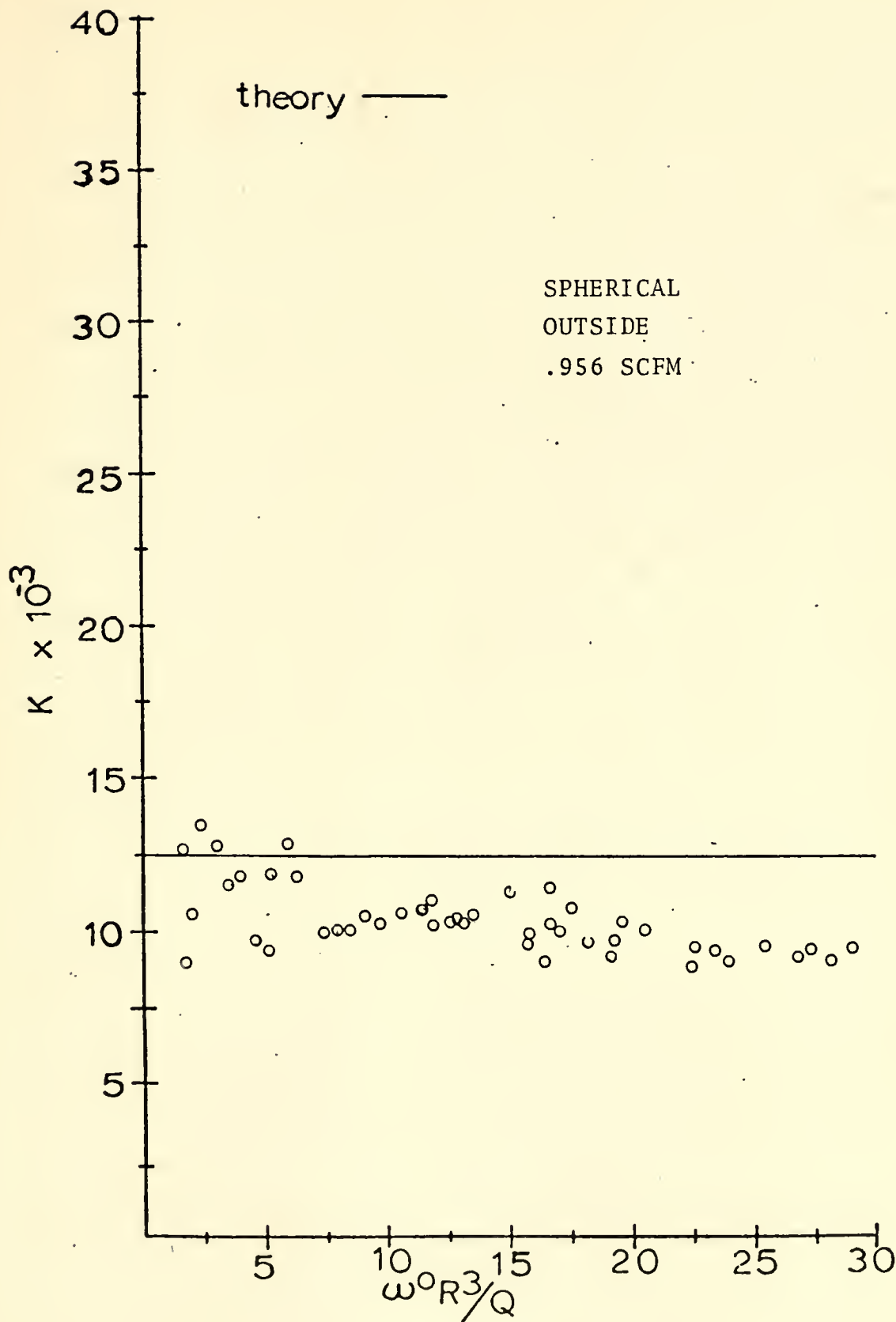


Figure 31. K vs. $\omega^0 R^3 / Q$ (outside spherical elements .956 SCFM).

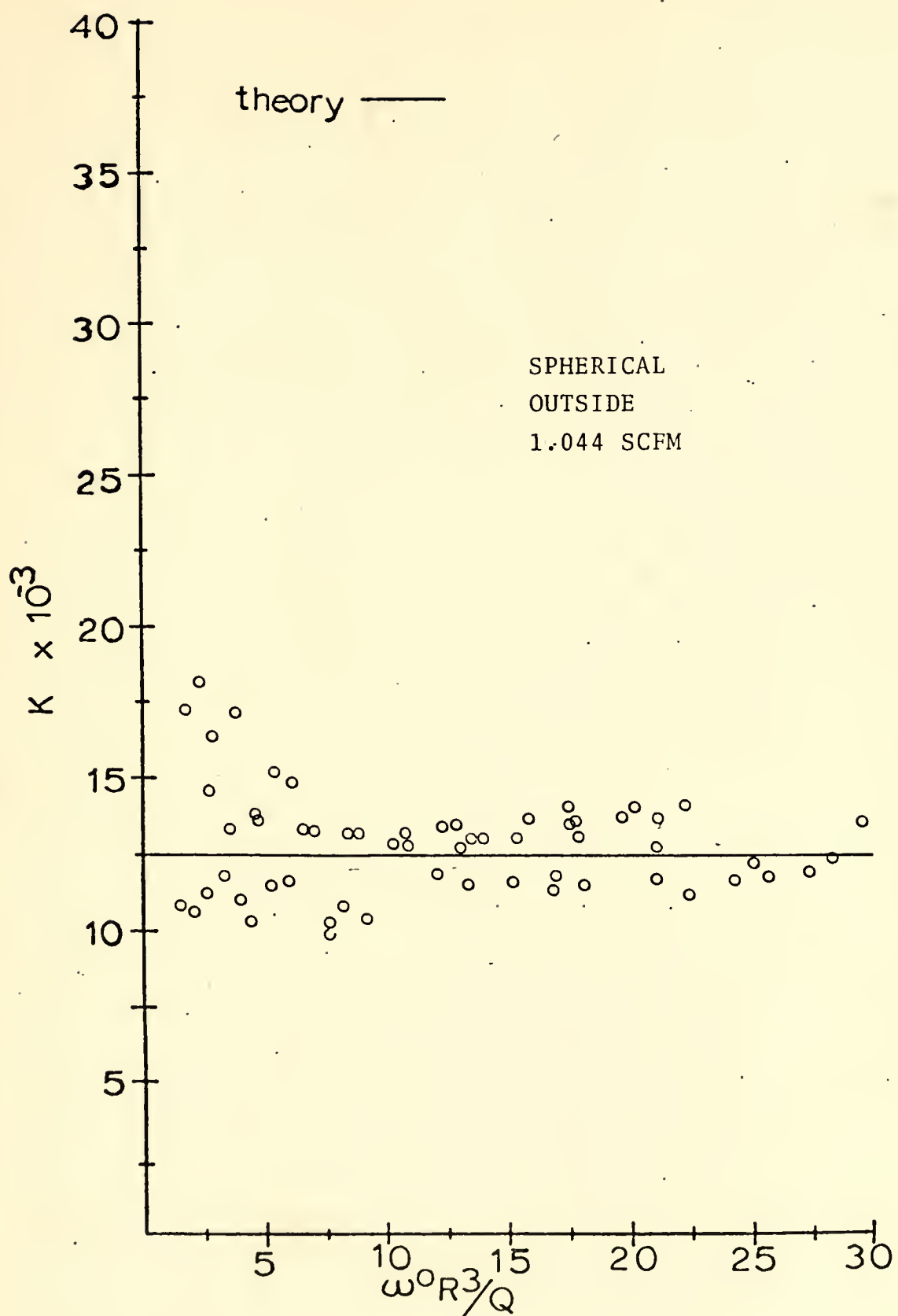


Figure 32. K vs. $\omega^0 R^3/Q$ (outside spherical elements 1.044 SCFM).

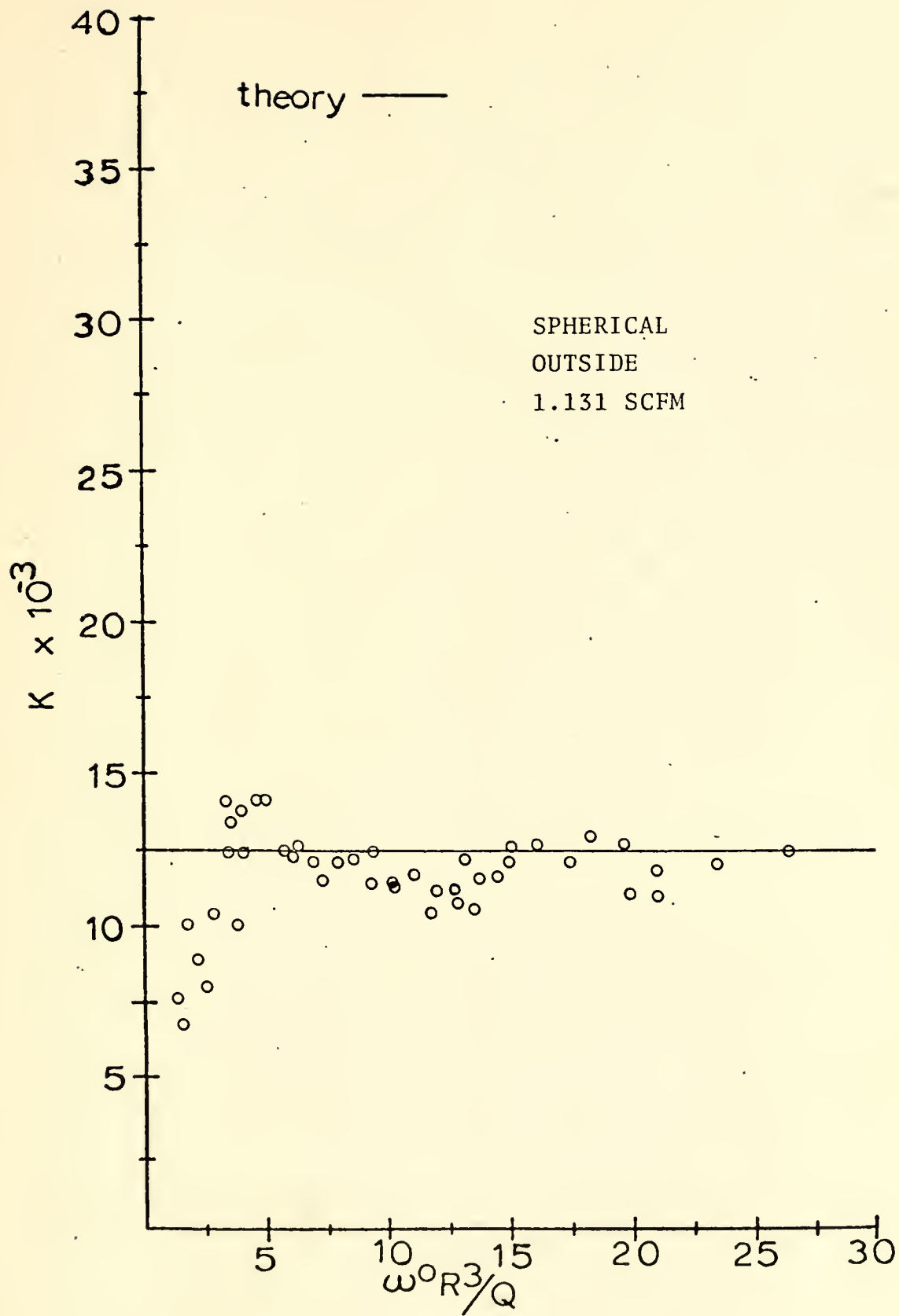


Figure 33. K vs. $\omega_0 R^3 / Q$ (outside spherical elements 1.131 SCFM).

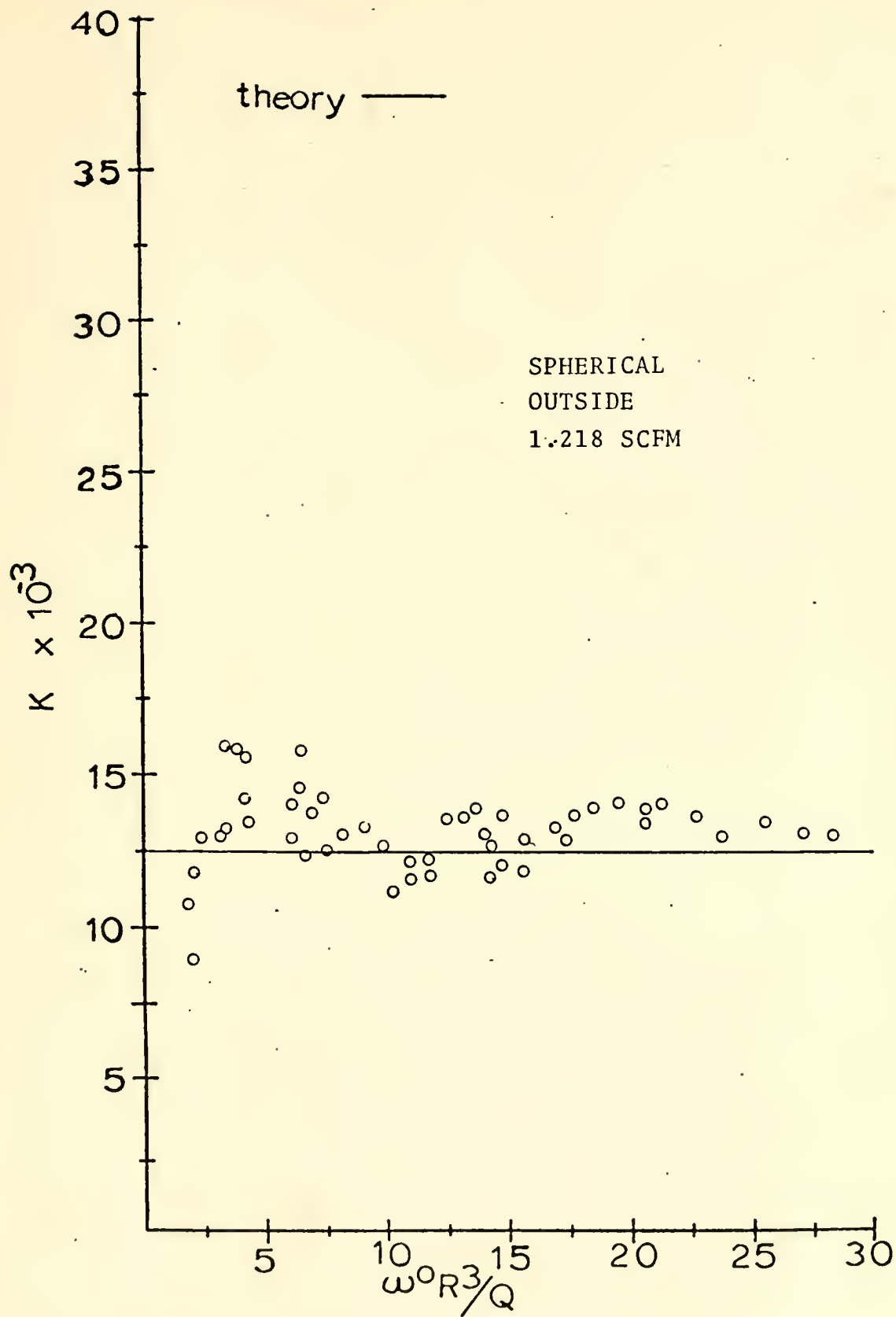


Figure 34. K vs. $\omega^0 R^3 / Q$ (outside spherical elements 1.218 SCFM).

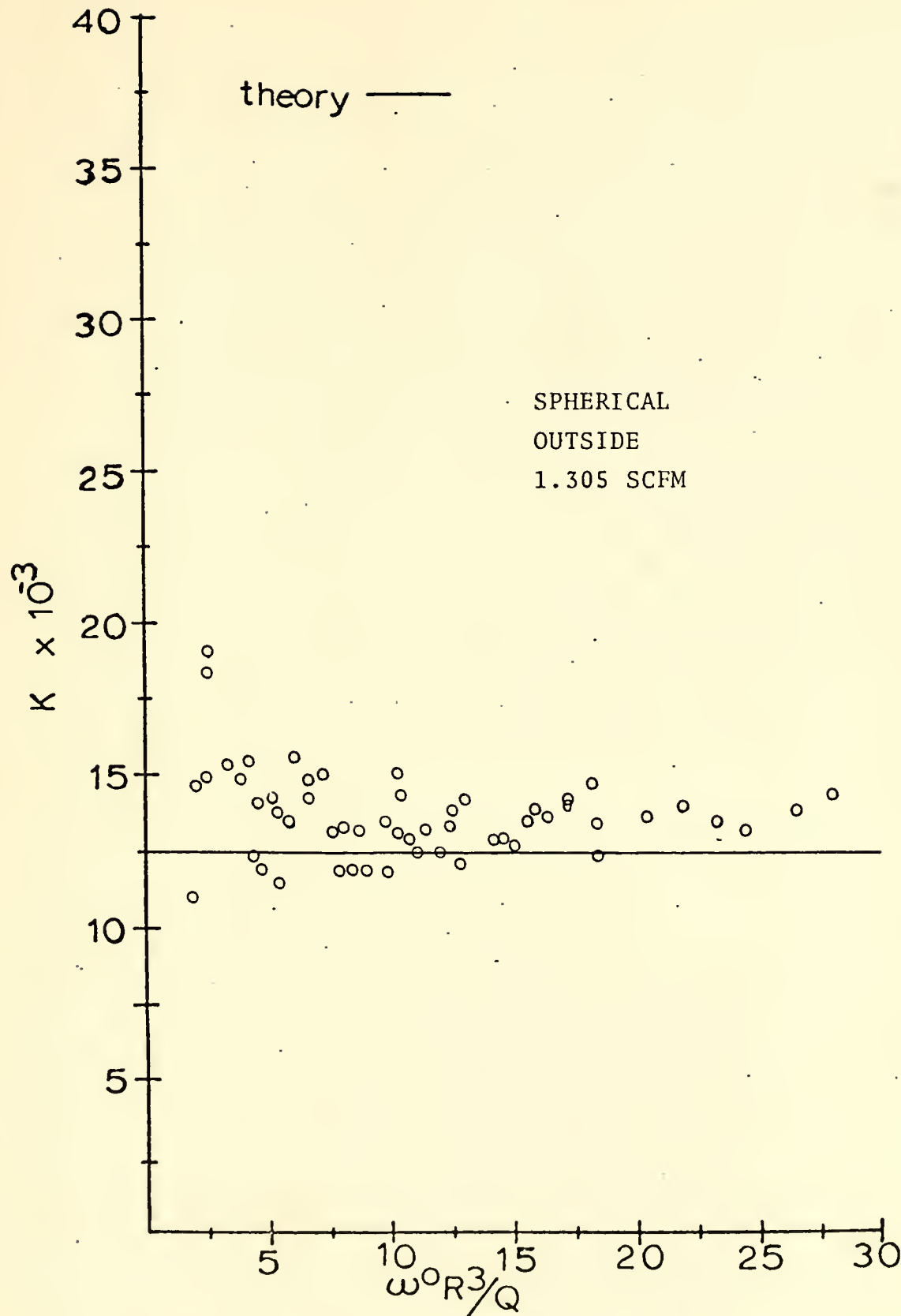


Figure 35. K vs. $\omega^0 R^3 / Q$ (outside spherical elements 1.305 SCFM).

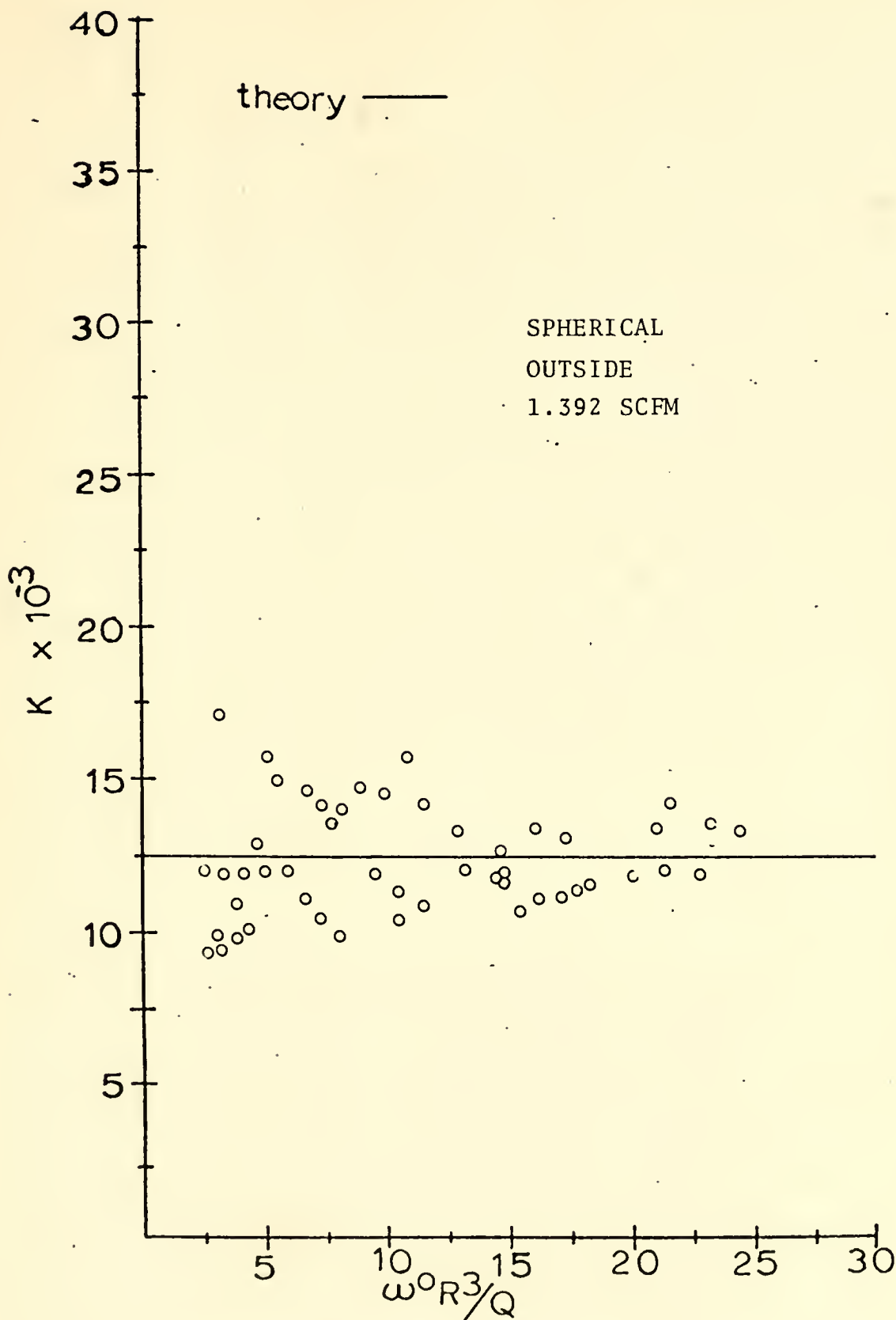


Figure 36. K vs. $\omega^0 R^3/Q$ (outside spherical elements 1.392 SCFM).

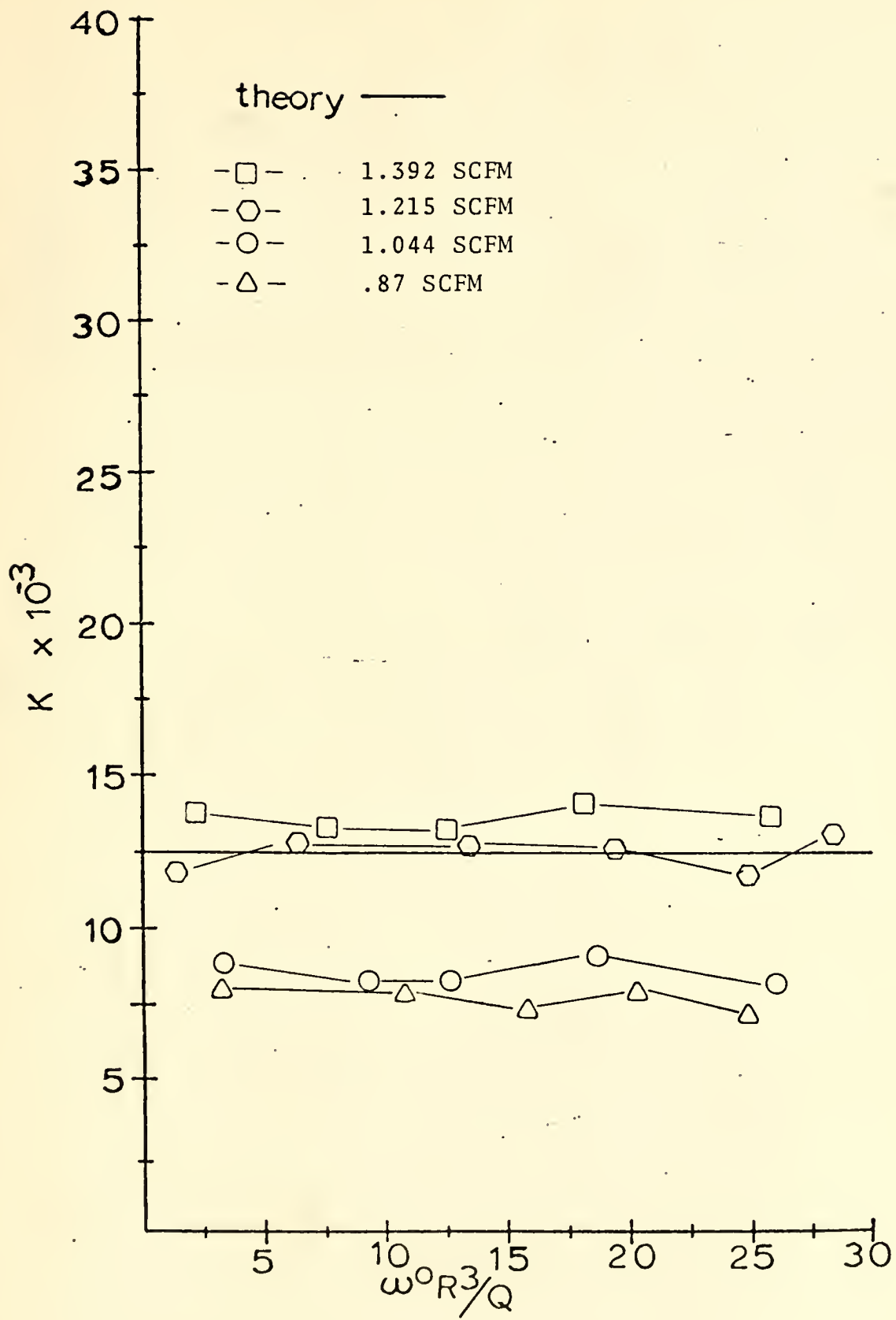


Figure 37. K vs. $\omega^0 R^3/Q$ (cylindrical element summary).

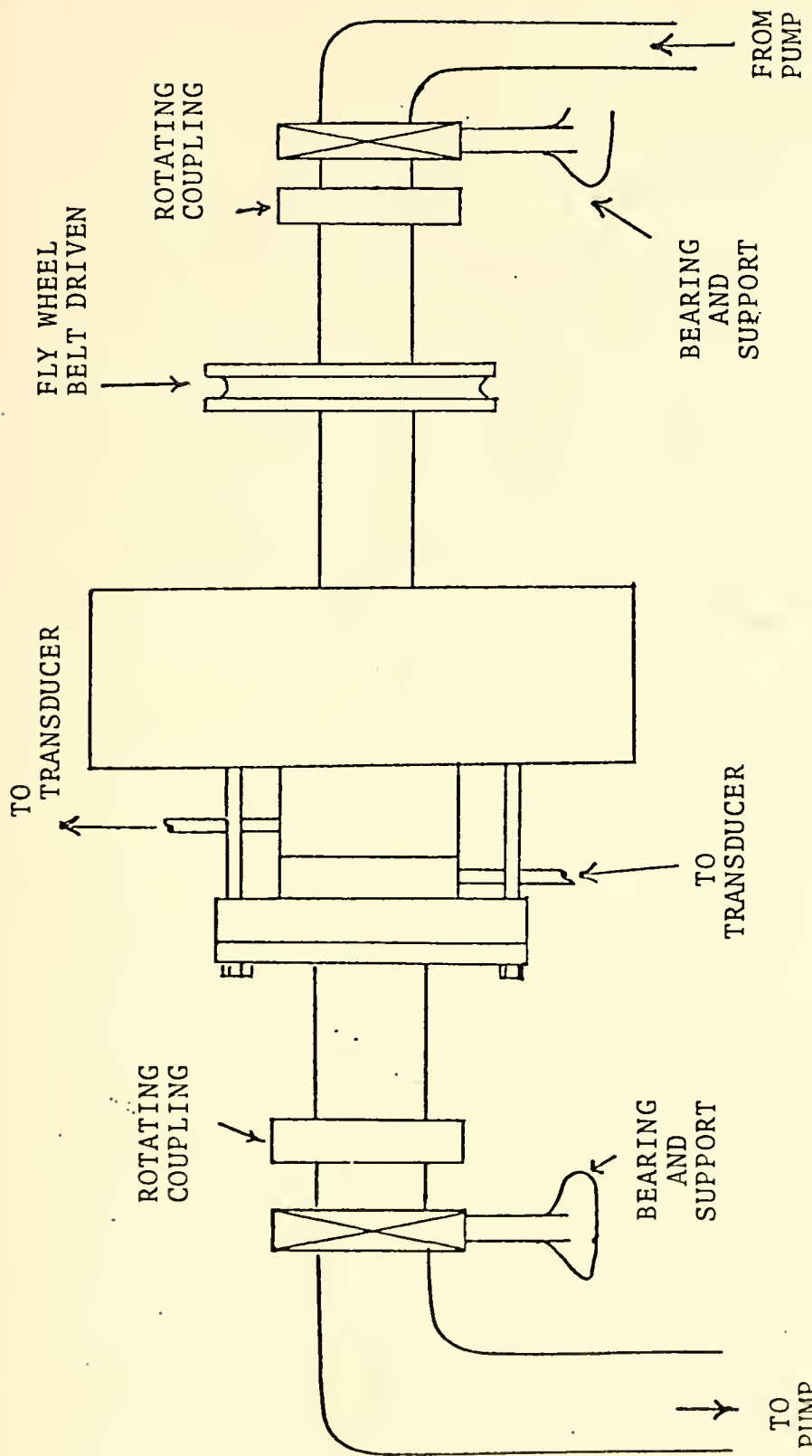


Figure 38. Prototype System.

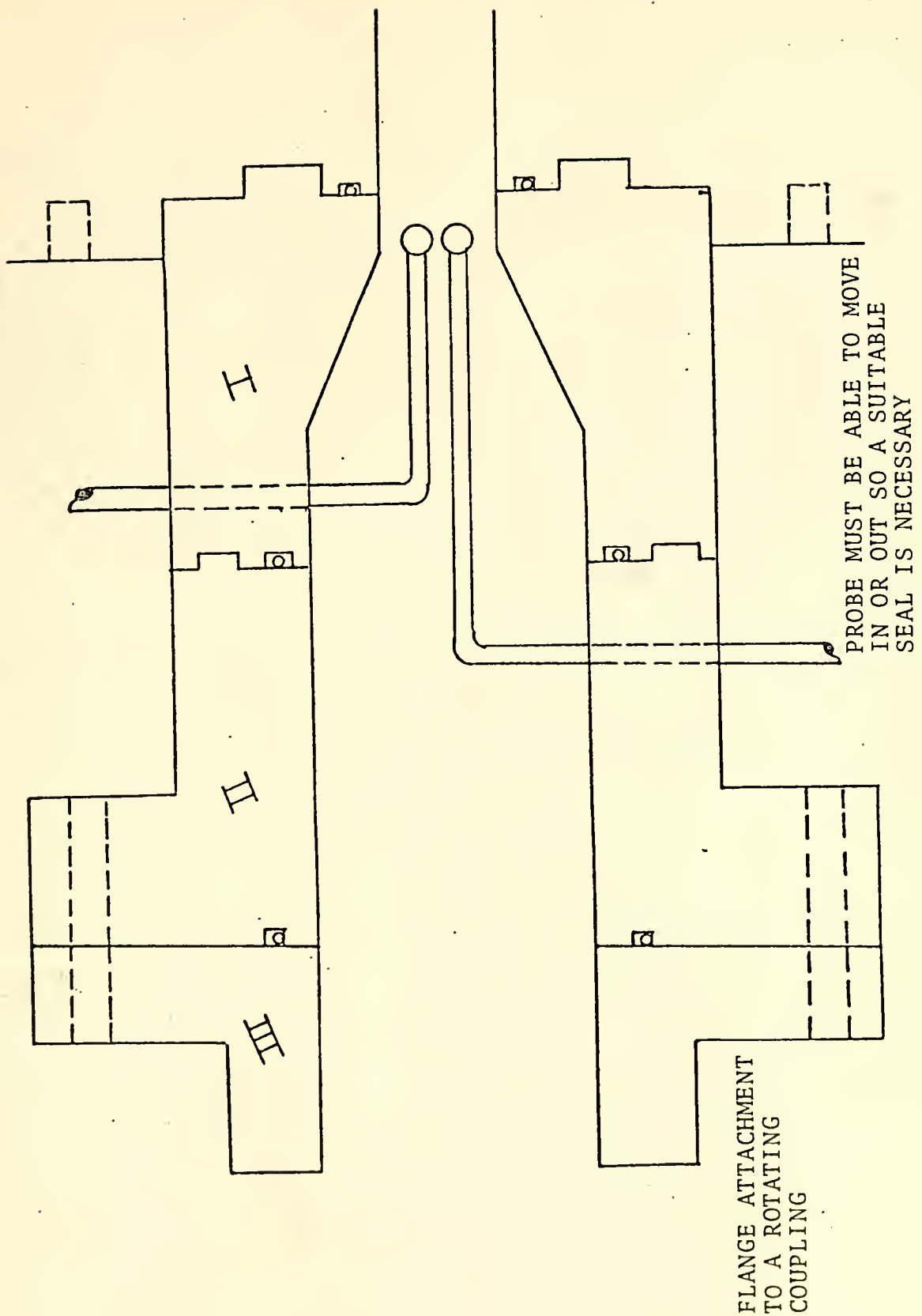


Figure 39. Prototype Pressure Sensor System.

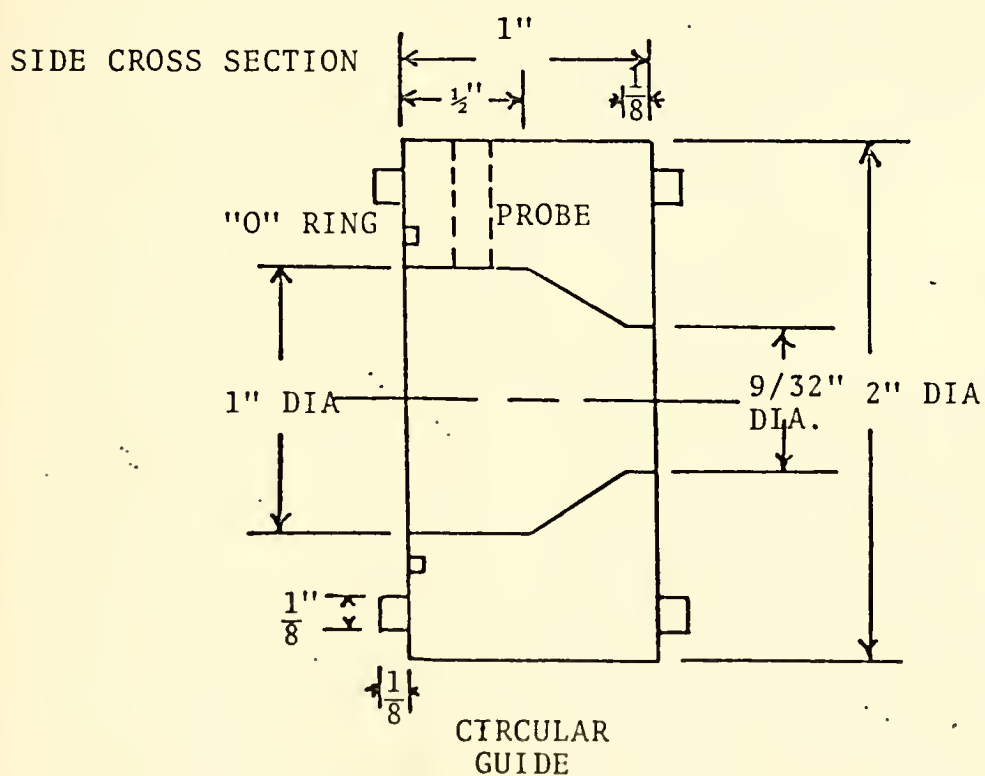
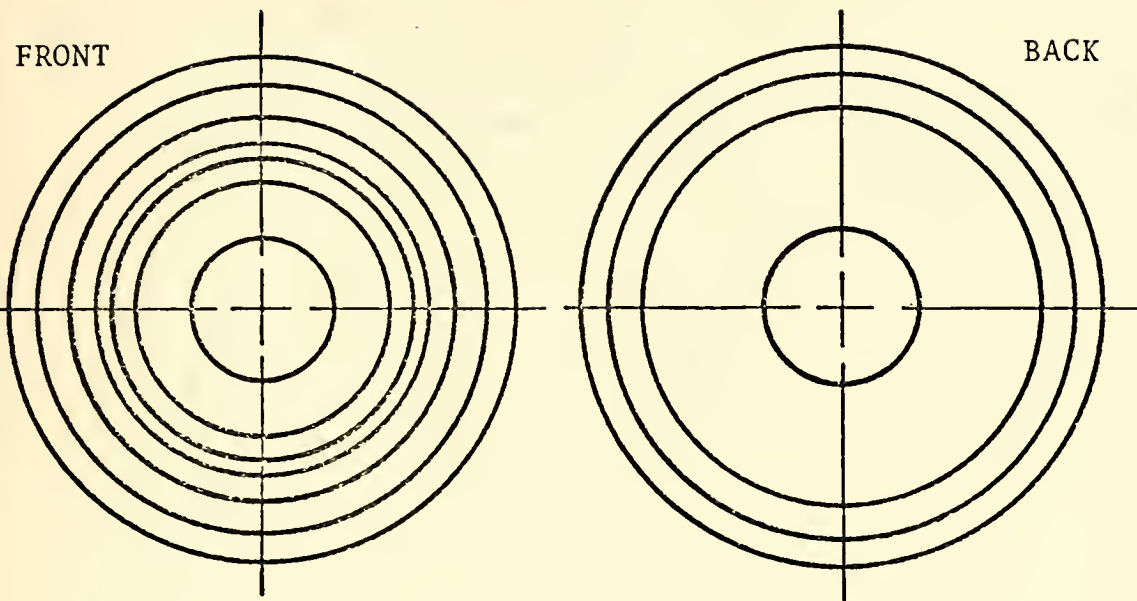


Figure 40. Pressure Sensor Section I.

II

FRONT

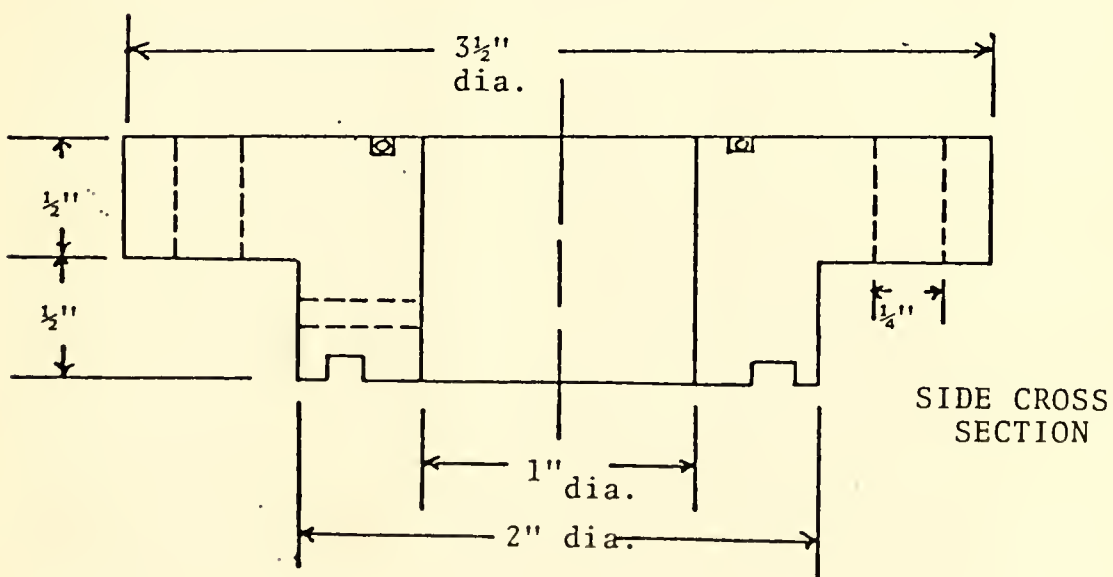
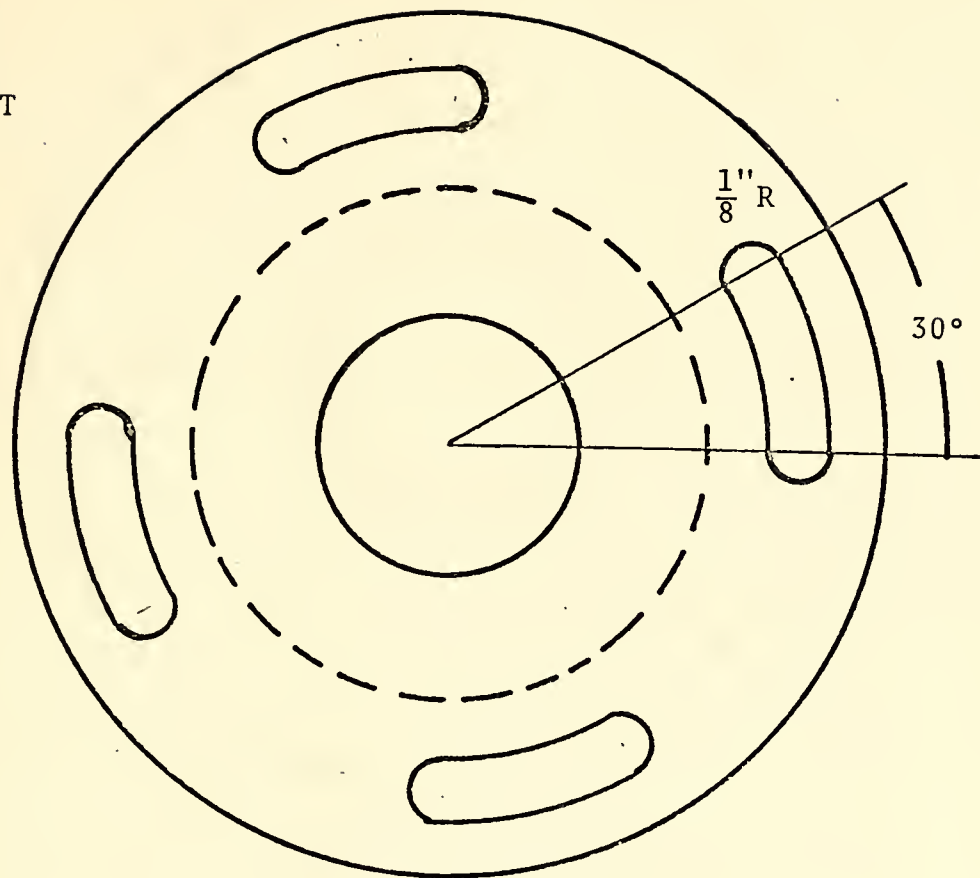
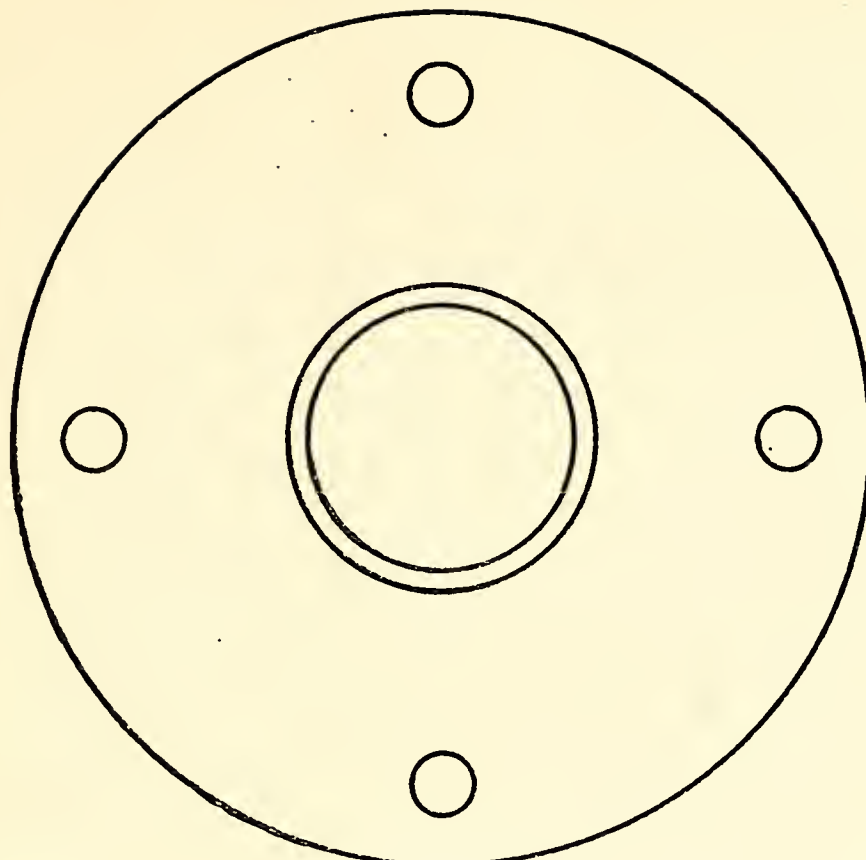


Figure 41. Pressure Sensor Section II.

III

FRONT



SIDE

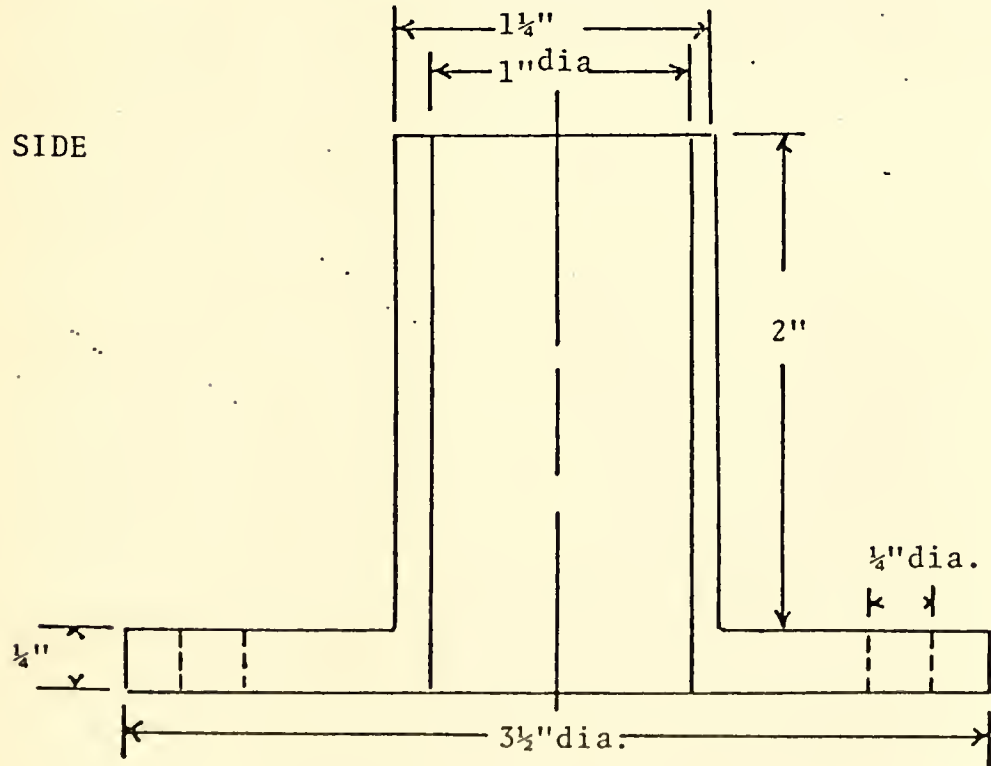


Figure 42. Pressure Sensor Section III.

SIDE VIEW

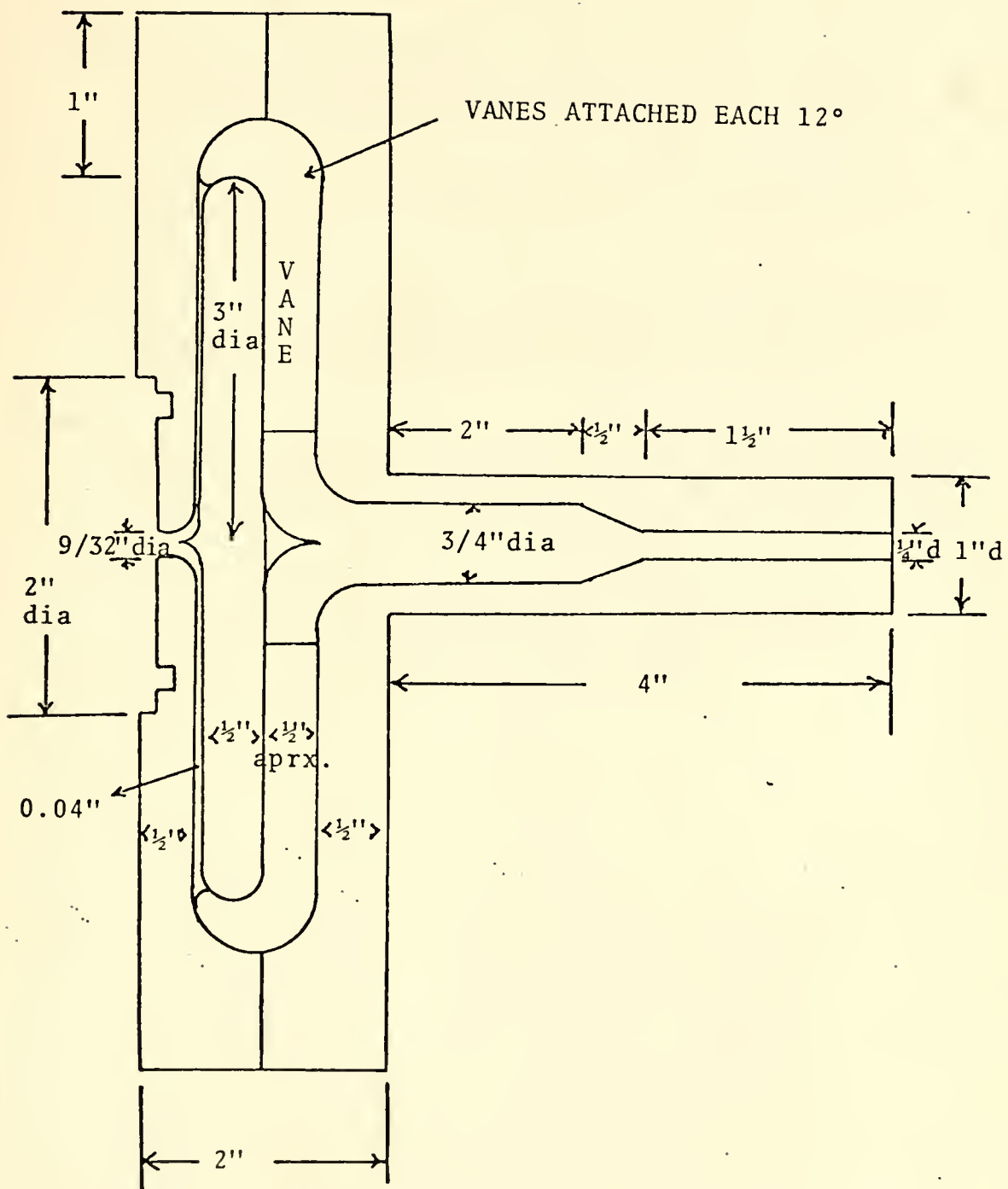


Figure 43. Sensor Assembly.

BIBLIOGRAPHY

1. Sarpkaya, T. and Kershner, J. M. and Gato, J. M., "A Theoretical and Experimental Study of Vortex Rate Gyro," Advances in Fluidics - The 1967 Fluidics Symposium, New York, ASME, p. 218-232,
2. Sarpkaya, T., "The Vortex Value and the Angular Rate Sensor," Fluidics Quarterly, vol. 1, p. 1-8, April 1968.
3. Richards, C. G., A Numerical Study of the Flow in the Vortex Angular Rate Sensor, paper presented at ASME Winter Annual Meeting, New York, N.Y., 29 November - 3 December 1970.
4. De Santes, M. J. and Rakowsky, E. L., An Experimental Investigation of the Viscous Flow Field in a Pneumatic Vortex Rate Sensor, paper presented at Fluidics Conference, Atlanta, Ga. 22-23 June 1970.
5. Iwadare, C., and Hakiwara, T., On Output and Supply Flows of an Angular Rate Sensor (in Japanese), Proceedings of the Japanese Fluid Amplification Symposium, vol. 1, p. 121-128, 1968.

THESIS DISTRIBUTION

	No. Copies
1. Defense Documentation Center Cameron Station Alexandria, Virginia 22314	2
2. Library, Code 0212 Naval Postgraduate School Monterey, California 93940	2
3. Chairman, Code 59 Department of Mechanical Engineering Naval Postgraduate School Monterey, California 93940	1
4. Professor T. Sarpkaya, Code 59 S1 Department of Mechanical Engineering Naval Postgraduate School Monterey, California 93940	1
5. LT D. B. Mulligan, USN 12206 Magnolia Blvd, #10 North Hollywood, Ca.	1

UNCLASSIFIED

Security Classification

DOCUMENT CONTROL DATA - R & D

(Security classification of title, body of abstract and indexing annotation must be entered when the overall report is classified)

1. ORIGINATING ACTIVITY (Corporate author) Naval Postgraduate School Monterey, California 93940	2a. REPORT SECURITY CLASSIFICATION Unclassified
	2b. GROUP

REPORT TITLE

AN EXPERIMENTAL STUDY OF THE PNEUMATIC ANGULAR RATE SENSOR

I. DESCRIPTIVE NOTES (Type of report and, inclusive dates)

Master's Thesis: June 1973

I. AUTHOR(S) (First name, middle initial, last name)

Daniel B. Mulligan; Lieutenant, United States Navy

1. REPORT DATE June 1973	2a. TOTAL NO. OF PAGES 70	2b. NO. OF REFS 5
3a. CONTRACT OR GRANT NO.	3b. ORIGINATOR'S REPORT NUMBER(S)	
4. PROJECT NO.		
5.	6b. OTHER REPORT NO(S) (Any other numbers that may be assigned this report)	
6.		
10. DISTRIBUTION STATEMENT		

Approved for public release; distribution unlimited.

11. SUPPLEMENTARY NOTES	12. SPONSORING MILITARY ACTIVITY Naval Postgraduate School Monterey, California 93940
-------------------------	---

13. ABSTRACT

The purpose of this investigation was to determine the response of a pneumatic angular rate sensor with two spherical pickoff elements, and to develop a suitable prototype sensor to be used in further analysis and experimentation. It was found that optimum response is obtained when the spherical elements are located within the sink tube, and that in the development of a suitable prototype, a fluid of relatively high density with low flow rates should be used to minimize system noise while retaining high system response.

~~UNCLASSIFIED~~

Security Classification

KEY WORDS	LINK A		LINK B		LINK C	
	ROLE	WT	ROLE	WT	ROLE	WT
ANGULAR RATE SENSOR						
PNEUMATIC						
SPHERICAL PICKOFF ELEMENTS						



Thesis
M8925 Mulligan 145032
c.1 An experimental study
of the pneumatic angular
rate sensor.

Thesis
M8925 Mulligan 145032
c.1 An experimental study
of the pneumatic angular
rate sensor.

thesM8925

An experimental study of the pneumatic a



3 2768 001 92538 1

DUDLEY KNOX LIBRARY